Geoscience Frontiers xxx (2016) 1–23

HOSTED BY

ELSEVIER

Contents lists available at ScienceDirect

China University of Geosciences (Beijing)

Geoscience Frontiers

journal homepage: www.elsevier.com/locate/gsf

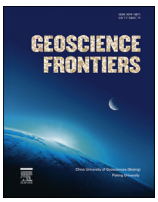

Research Paper

Alakit and Daldyn kimberlite fields, Siberia, Russia: Two types of mantle sub-terranes beneath central Yakutia?

I.V. Ashchepkov [a,*], A.M. Logvinova [a], T. Ntaflos [b], N.V. Vladykin [c], S.I. Kostrovitsky [c], Z. Spetsius [d], S.I. Mityukhin [d], S.A. Prokopyev [d], N.S. Medvedev [e], H. Downes [f]

[a] Institute of Geology and Mineralogy SD RAS, Koptyug Ave. 3, Novosibirsk, Russia
[b] Institute of Geochemistry SD RAS, Irkutsk, Russia
[c] Dept. of Lithospheric Research, University of Vienna, Althanstrasse 14, 1090 Vienna, Austria
[d] Alrosa Stock Company, ul. Lenina, 6, Mirny, Russia
[e] Nikolaev Institute of Inorganic Chemistry 3, Acad. Lavrentiev Ave. 3, Novosibirsk, 630090, Russia
[f] Department of Earth and Planetary Sciences, Birkbeck University of London, London, UK

ARTICLE INFO

Article history:
Received 29 December 2015
Received in revised form
1 August 2016
Accepted 18 August 2016
Available online xxx

Keywords:
Thermobarometry
Geochemistry
Daldyn
Alakit
Craton
Lithosphere

ABSTRACT

Mineral data from Yakutian kimberlites allow reconstruction of the history of lithospheric mantle. Differences occur in compositions of mantle pyropes and clinopyroxenes from large kimberlite pipes in the Alakit and Daldyn fields. In the Alakit field, Cr-diopsides are alkaline, and Stykanskaya and some other pipes contain more sub-calcic pyropes and dunitic-type diamond inclusions, while in the Daldyn field harzburgitic pyropes are frequent. The eclogitic diamond inclusions in the Alakit field are sharply divided in types and conditions, while in the Daldyn field they show varying compositions and often continuous Pressure–Temperature (P–T) ranges with increasing $Fe^{\#}$ with decreasing pressures. In Alakit, Cr-pargasites to richterites were found in all pipes, while in Daldyn, pargasites are rare Dalnyaya and Zarnitsa pipes. Cr-diopsides from the Alakit region show higher levels of light Rare Earth Elements (LREE) and stronger REE-slopes, and enrichment in light Rare Earth Elements (LREE), sometimes Th-U, and small troughs in Nb-Ta-Zr. In the Daldyn field, the High Field Strength Elements HFSE troughs are more common in clinopyroxenes with low REE abundances, while those from sheared and refertilized peridotites have smooth patterns. Garnets from Alakit show HREE minima, but those from Daldyn often have a trough at Y and high U and Pb. PTXfO_2 diagrams from both regions show similarities, suggesting similar layering and structures. The degree of metasomatism is often higher for pipes which show dispersion in P–$Fe^{\#}$ trends for garnets. In the mantle beneath Udachnaya and Aykhal, pipes show 6–7 linear arrays of P–$Fe^{\#}$ in the lower part of the mantle section at 7.5–3.0 GPa, probably reflecting primary subduction horizons. Beneath the Sytykanskaya pipe, there are several horizons with opposite inclinations which reflect metasomatic processes. The high dispersion of the P–$Fe^{\#}$ trend indicating widespread metasomatism is associated with decreased diamond grades. Possible explanation of the differences in mineralogy and geochemistry of the mantle sections may relate to their tectonic positions during growth of the lithospheric keel. Enrichment in volatiles and alkalis possibly corresponds to interaction with subduction-related fluids and melts in the craton margins. Incorporation of island arc peridotites from an eroded arc is a possible scenario.

1. Introduction

The most intensely studied kimberlite fields in the central part of the Yakutian kimberlite province (YKP) (Sobolev, 1977; Kostrovitsky et al., 2007) are the Daldyn and Alakit or Alakit-Markha fields according to the ALROSA division (Salikhov et al.,

* Corresponding author. Fax: +7 383 3332792.
E-mail addresses: Igor.Ashchepkov@igm.nsc.ru, garnet@igm.nsc.ru, igora57@mail.ru (I.V. Ashchepkov).
Peer-review under responsibility of China University of Geosciences (Beijing).

http://dx.doi.org/10.1016/j.gsf.2016.08.004

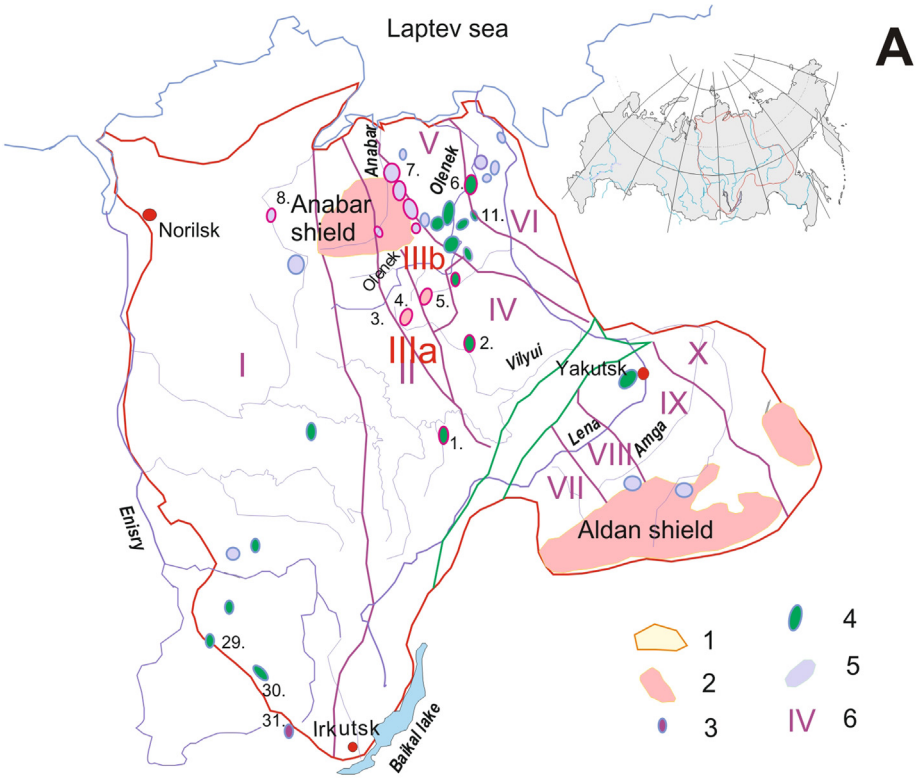

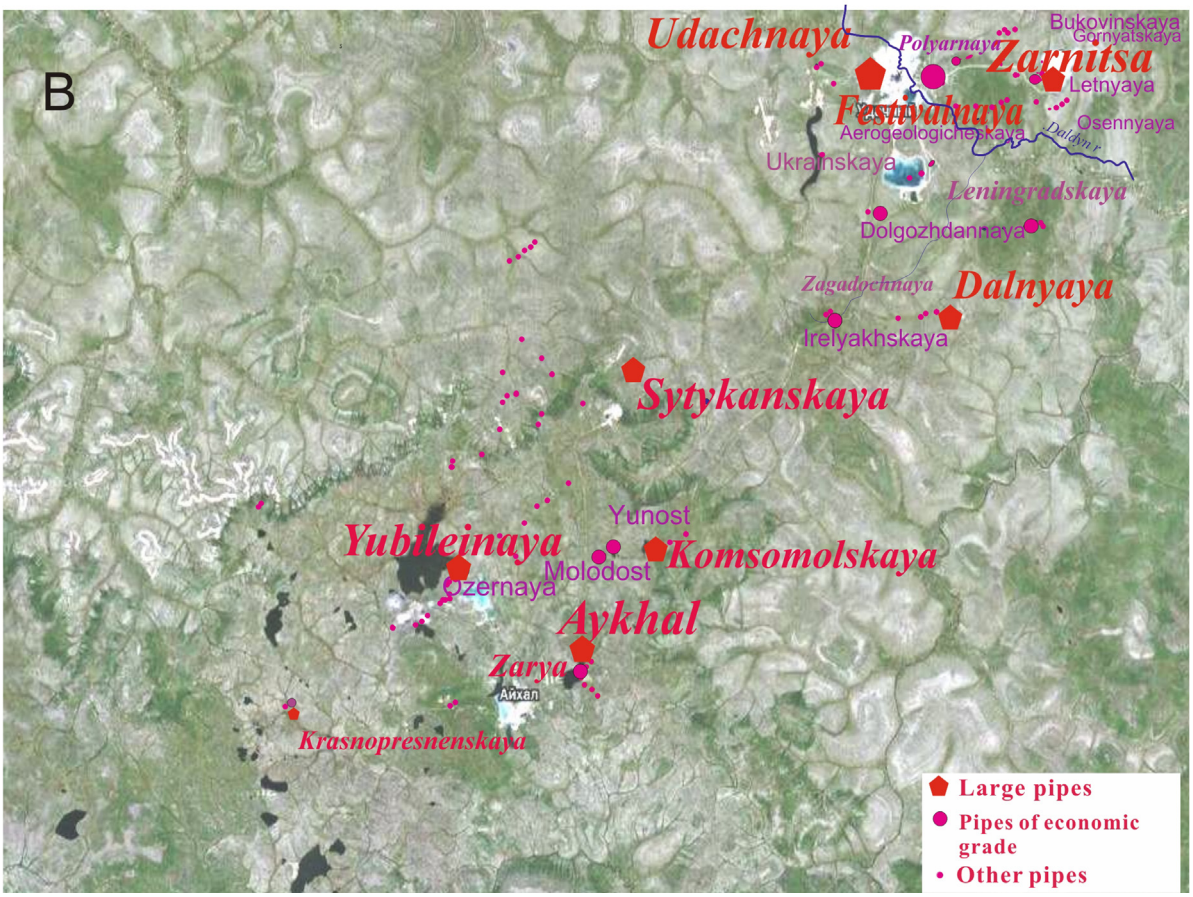

Figure 1. (A) The scheme of the Daldyn and Alakit field and their position on the Siberian craton. Fields: 1. Malo-Botuobinskoe, 2. Nakyn, 3. Alakit-Markha, 4. Daldyn, 5. Upper Muna, 6 and 7. Anabar field together (StarayaRechka, Ary-Mastakh, Dyuken, Luchakan, Kuranakh, Middle Koupnamka), 7. Kuoyka, 8. Kharamai. Terrains according to Gladkochub et al. (2006): I—Tungus; II—Magan; IIIa—West Daldyn; IIIb—East Daldyn; IV—Markha; V—Hapchan; VI—Birekte; VII–X—Aldan-Stanovoy province: VII—Olekma, VIII—Central Aldan, IX—East Aldan, X—Batomga. (B) Distribution of the large and small pipes in the Daldyn and Alakite fields.

Please cite this article in press as: Ashchepkov, I.V., et al., Alakit and Daldyn kimberlite fields, Siberia, Russia: Two types of mantle sub-terranes beneath central Yakutia?, Geoscience Frontiers (2016), http://dx.doi.org/10.1016/j.gsf.2016.08.004

2015). They both contain >50–80 kimberlite bodies (Fig. 1). Some large pipes such as Aykhal, Yubileynaya, Komsomolskaya and Sytykanskaya in the Alakit field and the Udachnaya, Zarnitsa and Dalnyaya pipes (Spetsius and Serenko, 1990) are being explored for diamonds. Some others like Zarya, Festivalnaya Leningradskaya, Irelyakhskaya, Dolgozhdannaya are also of economic grade. Smaller pipes commonly show lower diamond grades. Many scientific papers and studies have been devoted to the kimberlites, their mineralogy and mantle xenolith and xenocrysts (Pokhilenko et al., 1976, 1991, 1999, 2013; Sobolev, 1977; Rodionov et al., 1988; Ilupin et al., 1990; Spetsius and Serenko, 1990; Zinchuk et al., 1993; Boyd et al., 1997; Kuligin, 1997; Bulanova et al., 1998; Agashev et al., 2004, 2013; Pearson et al., 2005; Shatsky et al., 2008; Spetsius et al., 2008; Koreshkova et al., 2009; Nimis et al., 2009; Ashchepkov et al., 2010, 2013a,b, 2014a,b, 2015, 2016a,b; Ionov et al., 2010, 2011, 2013, 2015; Sobolev et al., 2011, 2015; Doucet et al., 2012, 2014; Alifirova et al., 2015 and reference there in).

The deep-seated material (xenoliths, megacrysts and xenocrysts) included in the kimberlites systematically vary in bulk and geochemical composition in these regions. However, systematic comparisons, including trace element geochemistry of the minerals, are lacking except for a fewer rather preliminary works (Sobolev, 1977; Spetsius and Serenko, 1990; Ashchepkov et al., 2013a,b).

All the pipes have nearly the same upper Devonian age of ~355–360 Ma (Agashev et al., 2004; Zaitsev and Smelov, 2010; Sun et al., 2014) except for Zagadochnaya which is of lower Triassic age (Zaitsev and Smelov, 2010).

Tectonically these two territories are divided into the West and East Daldyn terranes (Rosen et al., 2006), both belonging to the granulite-orthogneiss collision system. However, there are no great deep-seated faults dividing these two regions (Salikhov et al., 2015). According to tectonic reconstructions (Rosen et al., 2006), they are both located within the Paleoproterozoic Accretion Zone with a 1.8 Ma age corresponding to the peak of the Re/Os dates (Malkovets et al., 2012) for garnets and dating in other isotopic systems (Rosen et al., 2006) and for lower crust samples (Koreshkova et al., 2009). A preliminary estimation of the mantle layering and trace element geochemistry of the corresponding mantle melts showed that all mantle terranes within the YKP have their distinct features (Ashchepkov et al., 2013a,b, 2014a,b) as demonstrated an example of the typical mantle section beneath several pipes (Ashchepkov et al., 2010, 2012, 2013a, 2014a). Transects obtained using the approximation of the data along the profile from NE to SW show similarities in the mantle sections beneath all Alakit-Daldyn fields (Ashchepkov et al., 2014a,b) (Fig. 14). But the degree of depletion in the lower part became higher in Alakit in the lower part of the sub-cratonic lithospheric mantle (SCLM) just at the interval from Zagadochnaya (Nimis et al., 2009) to Sytykanskaya (Ashchepkov et al., 2015), with quite different mineralogy of mantle minerals and structure of SCLM. Here we present more detailed mineral geochemistry compared to the previous information (Ashchepkov et al., 2010, 2013a) and discuss the origin of the compositional differences of mantle sub-terranes and lithosphere structure.

2. Samples

Most of the studied samples were collected during fieldwork for joint research projects with ALROSA stock company in 2003–2007 and further cooperative works in the quarries of the large kimberlite pipes Udachnaya, Zarnitsa, Dalnyaya, Komsomolskaya and Yubileynaya, and in the ore stores of Sytykanskaya and other pipes. Heavy minerals concentrate from the kimberlites or drilling mud from the cores. Many heavy mineral separates were prepared from the kimberlite samples in Institute of Geochemistry (Irkutsk). For several pipes from Alakit and Daldyn fields, samples and concentrates were received from the ALROSA Company.

3. Methods

Samples were analyzed by standard methods. Mineral grains (~15,000) from mantle xenoliths from large pipes and xenocrysts of orthopyroxenes (Opx), clinopyroxenes (Cpx), garnets (Gar), olivine (Ol), chromite (Chr), ilmenite (Ilm) and amphiboles (Amph) from many other pipes were analyzed in Analytic Centre of IGM SD RAS, Novosibirsk.

Compositions were mostly determined using a CamebaxMicro electron microprobe (EMPA) in SB RAS using 15 kV acceleration voltage and 15 nA beam current in epoxy mounts of the polished mineral grains according to the procedure of Lavrent'ev and Usova (1994), Lavrent'ev et al. (1987). Compositions of some grains were determined using the Jeol Superprobe electron microprobe in Analytic Centre IGM. The relative standard deviation does not exceed 1.5%; the precision was close to 0.02–0.01% for minor elements. In addition mineral grains from ~340 xenoliths from Udachnaya, Sytykanskaya, Dalnyaya, Komsomolskaya, Yubileynaya pipes were determined in Vienna University. Detailed works on xenoliths in thin sections were conducted at the University of Vienna using a Cameca 100 SX microprobe with similar techniques but longer counting time (4 min) and a 2× improvement in precision. All analyses were obtained using mineral standards with wavelength-dispersive spectrometers; acceleration voltage and beam current were 15 kV and 20 nA, respectively, and standard correction procedures were applied.

Compositions of the trace elements for garnets and clinopyroxenes from Udachnaya (32), Zarnitsa (19), Dalnyaya pipe (15), and Aykhal (20) Yubileynaya (12), Sytykanskaya (25) Komsomolskaya (15) pipes were analyzed by LA-ICP-MS using a Finnigan Element I inductively coupled plasma mass spectrometer (ICPMS) with a Nd:YAG 193 UV New Wave laser system in the Analytic Centre IGM. The laser spot diameter did not exceed 10–20 μm. Scanning time for each grain was about 2.5–3 min. The concentrations of 32 trace elements were obtained and normalized to ^{40}Ca using EPMA values for silicate minerals. The relative standard deviations commonly were<5–8% and detection limit ranges from 10 to 20 ppb for REE, Ba, Th, U and large ion lithophile elements (LILE) and could exceed 10^{-8} for several trace elements. Analyses are represented in tables (Supplementary file 1). The trace element concentrations for minerals from Festivalnaya pipe were determined in Nikolaev Institute of Inorganic Chemistry SB RAS using quadrople ICPMS aniCAP Q (Thermo Scientific) and a New Wave Research NWR 213 nm Nd:YAG laser ablation system. This technique lets us to determine 32 trace elements with detection limits ranges from $n \times 10^{-5}$ to $n \times 10^{-7}$ wt.% and has standard deviation of the measurements ranges from 7 to 15%.

4. Chemical features of minerals in mantle xenolith and xenocrysts

4.1. Variations of mantle clinopyroxenes from Daldyn kimberlites

Clinopyroxenes from large Devonian pipes demonstrate similarities in their compositions. Peridotite minerals from the Udachnaya, pipe show rather low Na_2O concentrations in the MgO–Na_2O classification diagram. They are divided into the Mg-rich and Fe-enriched refertilized clinopyroxenes from deformed xenoliths (Ionov et al., 2010; Agashev et al., 2013), and Na-enriched Cpx from metasomatites related to the pyroxenitic type (Pokhilenko et al., 1999; Ashchepkov et al., 2013a,b). Diamond inclusions of peridotitic Cpx (Logvinova et al., 2005) are related to all types including metasomatized peridotites with very high Na-Cr content

Please cite this article in press as: Ashchepkov, I.V., et al., Alakit and Daldyn kimberlite fields, Siberia, Russia: Two types of mantle sub-terranes beneath central Yakutia?, Geoscience Frontiers (2016), http://dx.doi.org/10.1016/j.gsf.2016.08.004

(Pokhilenko et al., 1976). Cpx in eclogites from the Udachnaya pipe (Sobolev and Sobolev, 1993; Snyder et al., 1997; Sobolev et al., 1999; Pearson et al., 2005; Shatsky et al., 2008; Alifirova et al., 2015) are generally very enriched in Na_2O and Al_2O_3, but show rather wide variations in FeO (Fig. 2). In addition, omphacites from diamond eclogites and diamond inclusions (Bulanova et al., 1998; Sobolev et al., 2004; Logvinova et al., 2005) cover the entire compositional range. In the Dalnyaya pipe the range from depleted to enriched compositions is continuous, Na-enriched varieties are rare. Cr-diopsides from the Zarnitsa pipe display a more continuous range to Na-Al-rich metasomatic and pyroxenitic compositions. The difference between Fe- and Mg-types is not large. In the Festivalnaya pipe, the Fe-enriched but low-Na compositions similar to Cr-diopsides from Dalnyaya pipe prevail. Positive correlations for Fe-Ti and negative ones between Fe and Cr are common for all pipes except for Zarnitsa.

4.2. Variations of mantle clinopyroxenes from Alakit kimberlites

Cpx compositions from Aykhal show a division into highly Mg-rich and depleted (diamond associated group) (DG) in incompatible element groups and a strong increase in Na_2O (to 7 wt.%), starting mostly from the Fe-richgroups (FeG). Diamond-bearing eclogites correspond to group B and C of Dawson (1980) (Fig. 3).

In the Yubileynaya pipe, the Mg-content of Cpx is mostly intermediate in Fe but the increase of Na is even greater (Ashchepkov et al., 2004). In Komsomolskaya, the Mg–Na trend is discrete and diamond inclusions are related to the relatively Fe-enriched group. Cpx from diamond-bearing eclogites (Pernet-Fisher et al., 2014) belong to strongly enriched group B and C. Cpx from the Sytykanskaya pipe (Ashchepkov et al., 2015) show the most variable, trend and are also divided into DG and FeG groups and have a stepped trend of Na enrichment. Diamond inclusions of Cpx in these pipes belong to all groups and associations.

4.3. Variations of mantle garnets from Daldyn region

The garnet trends in the Cr_2O_3–CaO plot (Sobolev et al., 1973) for large pipes in Daldyn field are variable. A peridotite trend to 14 wt.% is quite definite for garnets from Udachnaya pipe belonging to diamond-bearing associations (Sobolev et al., 1984; Pokhilenko et al., 2013; Logvinova et al., 2005). Dunite and harzburgite associations show clusters in the sub-calcic field, TiO_2 enrichment also demonstrate some clustering. The Cr_2O_3–CaO trend for garnets from Dalnyaya is wider, possibly because many associations were initially harzburgitic and then were refertilized by reactions with melts. Harzburgitic trends are rather rare. The TiO_2 trend divides into two branches. The trend for garnets from the Zarnitsa pipe is flat to 6 wt.% Cr_2O_3 and then an increase in CaO occurs, due to the abundance of the pyroxenitic associations. Sub-calcic associations are more common from 4 wt.% Cr_2O_3, similar to Udachnaya, but the CaO content quickly decreases with Cr_2O_3. The amount of sub-Ca garnets in porphyritic kimberlites (PK) is higher than in autholithic breccia (ABK). The content of TiO_2 decreases with increasing Cr_2O_3. In Festivalnaya pipe the volume of sub-Ca and Cr-rich garnets is less than in the previously mentioned pipes (Fig. 4).

4.4. Variations of mantle garnets from Alakit region

In the Alakit field, garnets from the most productive Aykhal pipe show tight Cr_2O_3–CaO, and then the trend becomes scattered. Diamond inclusions in the sub-calcic field showing mostly dunitic affinity are very frequent. In Yubileynaya, the lherzolitic trend is more continuous. However, the sub-calcic field is widely represented starting from 8 to 6 wt.% Cr_2O_3. Pyrope diamond inclusions are not frequent in this pipe. The pyrope trend for the Komsomolskaya pipe is not very continuous and shifts to the pyroxenite field after 8 wt.% Cr_2O_3 (Fig. 5). The diamond inclusions are mostly harzburgitic and give a scattered plot (Sobolev et al., 2004; Logvinova et al., 2005). Garnet trends from Sytykanskaya pipe are also located mainly in the lherzolitic field with deviations to the pyroxenitic field in the middle part of diagram. Diamond inclusions (Spetsius and Koptil, 2008) are concentrated in the dunitic field and a few of them belong to the harzburgite and pyroxenite suites.

4.5. Mantle amphiboles

Amphiboles are common in the northern part of the mantle lithosphere beneath the YKP (Ashchepkov et al., 2016a,b), and mostly belong to the Cr-hornblende-pargasitic types. They were found also in the Alakit field. Most of them are from Yubileinaya pipe where they occur in depleted metasomatized harzburgite xenoliths (Ashchepkov et al., 2004). They contain notable amounts of Cr and range from pargasites to richterites, with continuous increases in K and Na (Fig. 6). Pargasitic amphiboles were found also in Sytykanskaya (Ashchepkov et al., 2015) and Komsomolskaya pipes. This is the first occurrence of amphiboles reported from the Daldyn field. Several were found in the rims surrounding garnets in Zarnitsa pipe. Intergranular pargasites were discovered in xenoliths from Dalnyaya pipe. Thin amphibole needles substitute for orthopyroxenes in harzburgites.

5. Thermobarometry

5.1. PTX conditions in mantle determined by single grain thermobarometry

In this study we present we made modifications to the previously published PTXfO_2 diagrams (Ashchepkov et al., 2012, 2013a, 2014a,b, 2015), adding analyses for eclogites and diamond inclusions.

5.1.1. PTXfO_2 diagrams for kimberlite pipes from Daldyn region

The diagram for the Udachnaya pipe was described in detail (Ashchepkov et al., 2010, 2014a,b). This mantle column is sharply layered and shows a rather wide range of temperatures in each level due to reactions with the intruded protokimberlite melts.

In the new version, the PTXfO_2 diagram is completed by more details for the eclogite associations (Alifirova et al., 2015). In the mantle column beneath this pipe, the eclogite associations very often follow the high temperature (HT) branch. They correspond to the diamond-graphite transition (GDT) coinciding in $Fe^{\#}$ with the megacryst associations or related to the deformed peridotites. The low temperature eclogites are close to the branch traced by the diamond inclusions or even more cold conditions ($\sim$33 mW/m^2). The more Fe-rich eclogite associations show trend of increasing of $Fe^{\#}$ with decreasing temperatures, which reach the highest values at 4–3.5 GPa. The Ca-Al-rich eclogites are distributed in the 5 to 6 GPa interval (Fig. 7A).

The mantle column beneath Zarnitsa also was described in detail (Ashchepkov et al., 2010, 2014a,b). The mantle structure beneath this pipe is similar to those determined for Udachnaya, but the PT plot is more scattered and layering is more dispersed. Among the xenoliths, several metasomatic associations with amphiboles were found, which are rare in Udachnaya. Eclogitic garnets (our data and from Alifirova et al., 2015) and several PT values for eclogites and diamond inclusions (Bulanova et al., 1998) complete the PTX diagram. The diamond inclusions are sub-calcic garnets related to the low temperature branch. The FeG are more Fe-rich than those from common sheared peridotites (Nixon and Boyd,

Please cite this article in press as: Ashchepkov, I.V., et al., Alakit and Daldyn kimberlite fields, Siberia, Russia: Two types of mantle sub-terranes beneath central Yakutia?, Geoscience Frontiers (2016), http://dx.doi.org/10.1016/j.gsf.2016.08.004

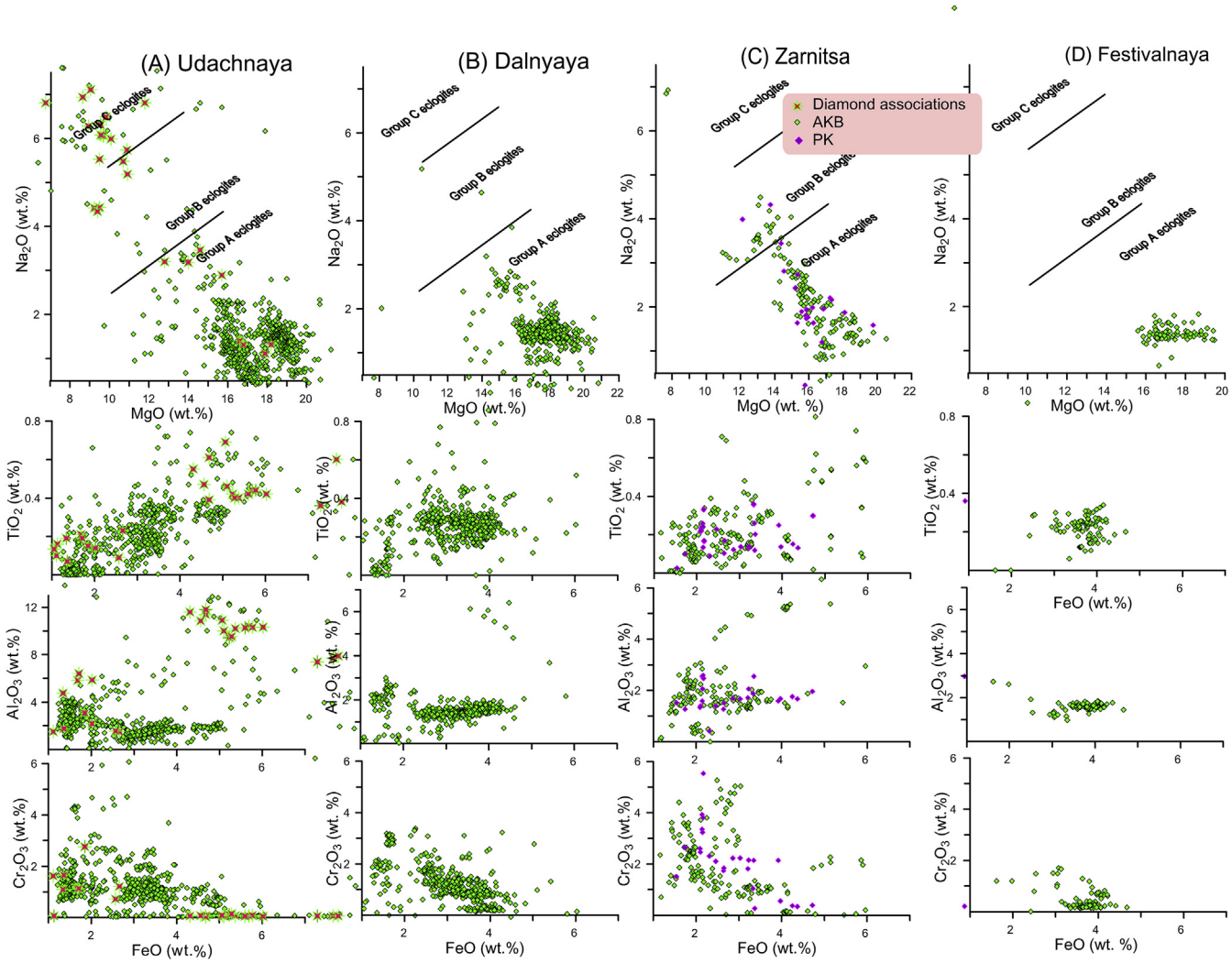

Figure 2. Variation diagrams for mantle clinopyroxenes from the most productive pipes in the Daldyn field. (A) Udachnaya; (B) Dalnyaya; (C) Zarnitsa; (D) Festivalnaya.

1973; Agashev et al., 2013) and probably belong to the megacryst associations. All eclogitic omphacites are located near the graphite-diamond transition. Eclogites found as xenoliths and xenocrysts are related to the relatively Mg-rich group and are slightly higher in $Fe^{\#}$ than the megacrysts. The garnets are close to the megacrystic associations and Mg-type eclogite common geotherm from the bottom of mantle section to 3.3 GPa, which is the upper boundary for the megacrysts (Fig. 7B). Xenocrysts of eclogitic garnets show joint increase of Ca and Fe at the pressure ranging from 2.5 to 6.0 GPa.

A separate diagram based on analyses of xenocrysts from the PK from Zarnitsa pipe reveals a simpler and more contrasted layering with fluctuations of $Fe^{\#}$ for Gar from 0.05 to 0.11. The ilmenite trend demonstrates a smooth increase of $Fe^{\#}$ and Cr content (from 4 GPa) with decreasing pressure starting from the LBA (lithosphere-asthenosphere boundary) to 3 GPa, and clustering into 4 groups (Fig. 7E).

For the Dalnyaya pipe, the mantle structure was determined for xenocrysts from autholithic kimberlite breccia (AKB) and porphyritic kimberlite (PK) (Ashchepkov et al., 2016b). The wide set of analyzed xenoliths (~160) shows that most of mantle column was reacted from the bottom and was subjected to very intense metasomatism. The mantle column has been relatively homogenized by the reactions and the layering is not seen in detail. In the SCLM beneath Dalnyaya, the lower part of the mantle section is strongly heated and many clinopyroxenes are low-Cr and belong to the megacrystalline associations found in intergrowths with ilmenites (Rodionov et al., 1988) (Fig. 7C). Sub-calcic garnets and chromites as diamonds were found in the bottom and in middle part of the mantle sections.

The mantle column beneath the Festivalnaya pipe reveals a generally similar situation, but with layering not so evident compared to Udachnaya. In the lower part of the mantle sections, the double P–$Fe^{\#}$ trends for the garnets and cold split geotherm are the most distinct features. The hot branch is mainly represented by Fe-rich Gar and low-Cr FeG Cpx, which demonstrates an increase from the LBA to 3.5 GPa, with slightly increasing $Fe^{\#}$ from 0.11 to 0.15, forming the megacrystalline trend together with the ilmenites trend which is also more Fe-rich (Fig. 7D).

5.1.2. *PTXfO_2 diagrams for kimberlite pipes from Alakit region*

The PTX diagram for Yubileinaya shows three large intervals. All Cr-diopsides are higher in Fe. Some Fe-rich and low-Cr Cpx belong to the megacrystic type (Kopylova et al., 2009), the garnet of low-Cr type display PT estimates forming a trend parallel to the ilmenite megacrysts. The eclogitic garnets display a trend from the base of the lithosphere to the middle of the SCLM with increasing $Fe^{\#}$ (Fig. 8A).

Please cite this article in press as: Ashchepkov, I.V., et al., Alakit and Daldyn kimberlite fields, Siberia, Russia: Two types of mantle sub-terranes beneath central Yakutia?, Geoscience Frontiers (2016), http://dx.doi.org/10.1016/j.gsf.2016.08.004

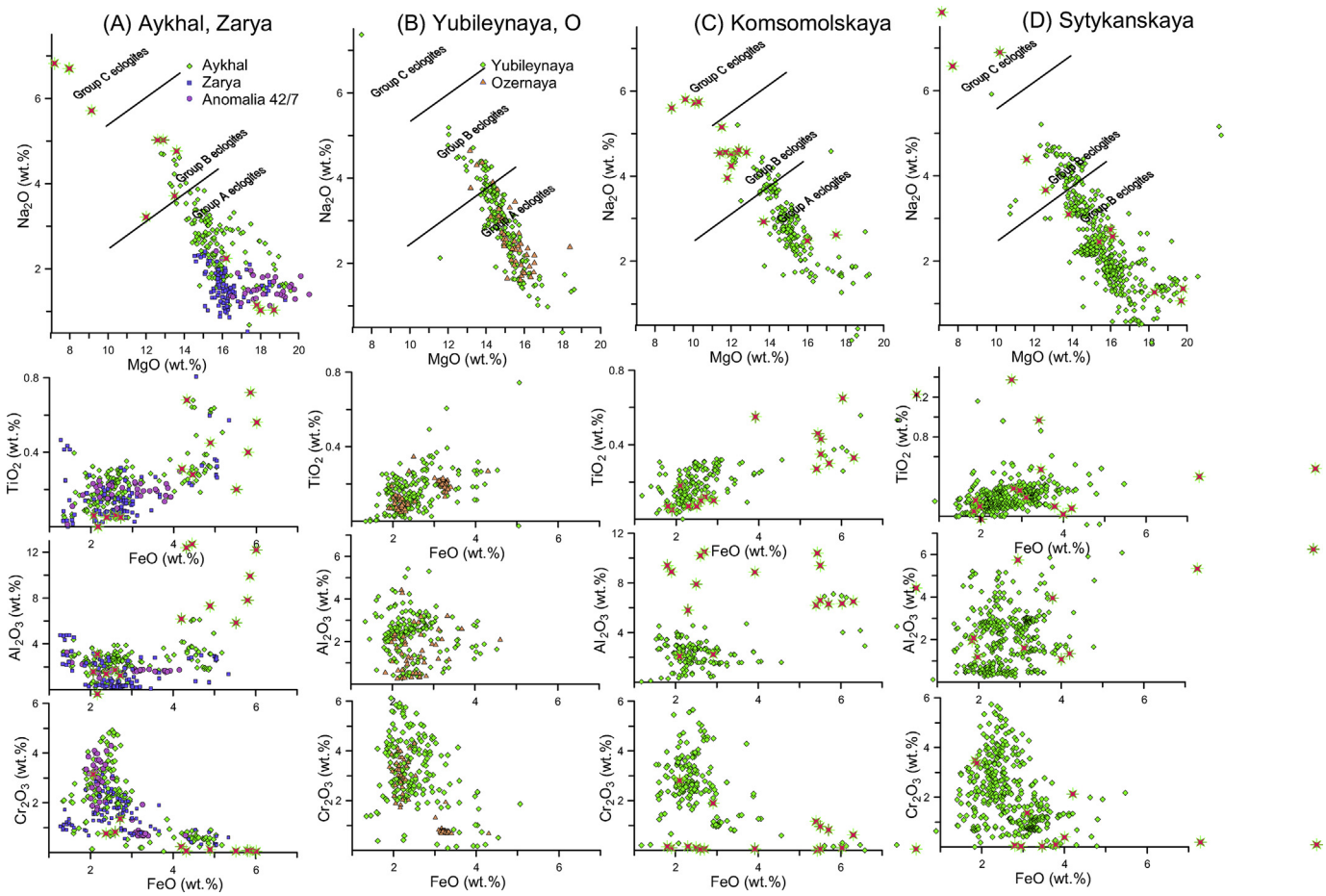

Figure 3. Variation diagrams for mantle clinopyroxenes from the most productive pipes in the Alakit field. (A) Aykhal and Zarya; (B) Yubileinaya; (C) Komsomolskaya; (D) Sytykanskaya.

The diagram for Komsomolskaya pipe was completed by P–T estimates for diamond-bearing eclogites (Pernet-Fisher, 2013), which show three clusters from the base of the lithosphere to GDT boundary. The Ca-rich varieties are located in the lower part of mantle section as beneath Udachnaya (Fig. 8B).

The diagram for the Komsomolskaya pipe was completed by the PT estimates for diamond-bearing eclogites (Pernet-Fisher et al., 2013) which show three trends from the base of the lithosphere to the graphite-diamond transition. The Ca-rich varieties are located in the lower part of the mantle section, as beneath Udachnaya (Fig. 8B).

The diagram for the SCLM from Sytykanskaya (Ashchepkov et al., 2015) was also completed with P–T estimates for almandine-pyrope diamond inclusions. They generally show distributions similar to those found for the Komsomolskaya pipe, but are more Mg-Ca-rich and belong to the deeper level near the base of the lithosphere. The pyrope diamond inclusions of dunitic type (Stachel and Harris, 2008) also belong to the lithosphere base (Fig. 8C).

The mantle structure beneath the Aykhal pipe is sharply layered and shows a continuous increase of Fe from the base of the lithosphere to the Moho with similar arrays of P–Fe$^{\#}$ in 6 to 7 major intervals of pressure. The high temperature ilmenite-clinopyroxene stepped trend traces five intervals from the base of the lithosphere to 2.5 GPa. Garnet diamond inclusions split into the cold and hot branches, as well in Fe$^{\#}$ (Fig. 8D).

The PTX diagram for the satellite pipe Zarya reveals similar but less contrasting layering, Garnets in the middle and upper part of the SCLM are mostly more Fe-rich. The trend for the megacrystic pyropes with Fe$^{\#}$ from 0.11 to 0.13 rises from the LBA to 2.5 GPa. The ilmenite trend is denser in the lower part compared to the Aykhal pipe (Fig. 8E).

The oxidation state determined for the mantle columns beneath the Alakite and Daldyn fields by garnets mainly relates to the primary conditions of SCLM, and does not differ much from other parts of Siberian and other cratons (McCammon et al., 2001).

5.2. The comparison of the Opx-based geotherms for the Daldyn and Alakit fields

In this paper we represent the Opx-based geotherms (T (°C Brey and Kohler, 1990)– P(GPa; McGregor, 1974)) and Opx-Gar thermobarometry (Brey and Kohler, 1990), considered to be the most reliable, and representing the primary P–T conditions in the SCLM because Cpx often characterizes regeneration processes. For all the pipes except Udachnaya, these data are quite new. Combinations of the single grain Opx PT (BK90Opx-MG74) values are close to the Opx-Gar thermobarometry (BK90) and show the conditions for fresh xenoliths, which are rare in all pipes except for Udachnaya. Our Gar-based thermobarometry (Ashchepkov et al., 2016a,b) (this volume) covering all the PT fields in the diagrams show PT range for all mantle associations (Fig. 9).

All pipes from Daldyn field have similarities and show stepped and split geotherms with repeated cooler and warmer areas in PT diagrams. The upper 3.0–1.0 GPa interval is much hotter than in the SCLM beneath Alakit. The evident high temperature convecting

Please cite this article in press as: Ashchepkov, I.V., et al., Alakit and Daldyn kimberlite fields, Siberia, Russia: Two types of mantle sub-terranes beneath central Yakutia?, Geoscience Frontiers (2016), http://dx.doi.org/10.1016/j.gsf.2016.08.004

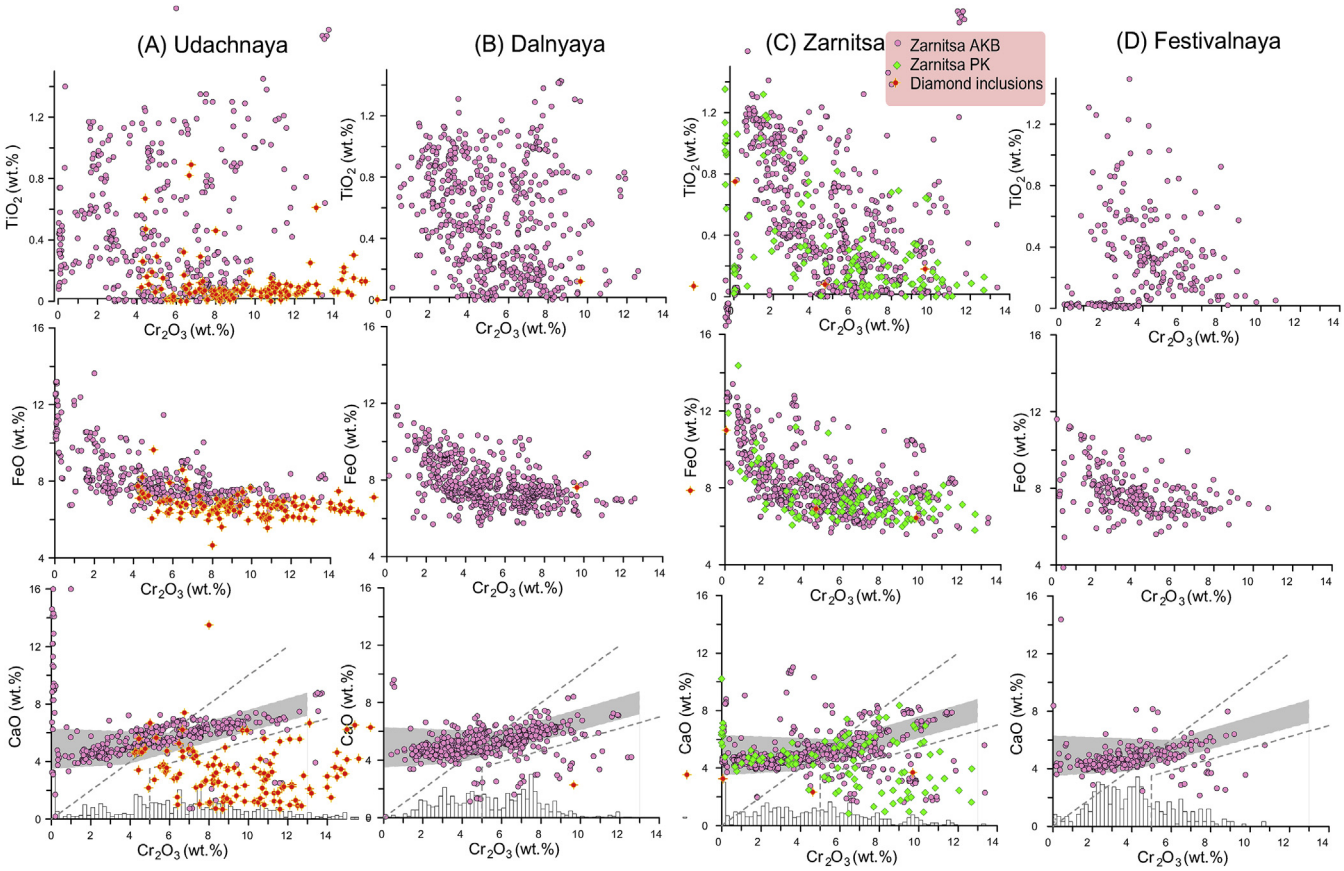

Figure 4. Variation diagrams for mantle garnets from the most productive pipes in the Daldyn field. (A) Udachnaya; (B) Dalnyaya; (C) Zarnitsa; (D) Festivalnaya.

branch (Boyd et al., 1997) related to the sheared peridotites found in Udachnaya (Agashev et al., 2013) is pronounced also for Dalnyaya and Zarnitsa pipes. The only example from Sytykanskaya shows a linear low temperature geotherm, which is colder than calculated for SCLM beneath the Udachnaya and Dalnyaya pipes. A few deviations to a high temperature geotherm are seen near the graphite-diamond transition and garnet-spinel transition. A very similar cold and smooth linear geotherm was produced using Cpx for the SCLM beneath Yubileinaya (Ashchepkov et al., 2004). These straight line and cold pyroxene geotherms are common for all SCLM beneath all large pipes in the Alakit field.

6. Geochemistry of mantle minerals

6.1. Trace elements in minerals from Daldyn field

The LA-ICPMS analyses were determined for minerals from all pipes. Clinopyroxenes from Udachnaya pipe (Ashchepkov et al., 2013b) show different patterns in each of the distinct groups. The trace element patterns for clinopyroxenes from lherzolites are mostly highly inclined with strong variations in the HREE, with varying $(La/Yb)_n$ ratios, and a small hump in the LREE (Fig. 10). Cpx from very depleted harzburgites show low concentrations of trace elements and concave REE patterns in the HREE part. They have deep Nb and Hf troughs while Cpx commonly shows deep Zr and moderate Ta-Nb anomalies. The spider diagrams for sheared peridotites show round REE and smoothed enriched patterns (Ionov et al., 2010; Agashev et al., 2013) with LREE-enrichment, Sr troughs and Pb peaks shown by some Gar-bearing varieties. Most peridotite garnets show Zr, Ba troughs as well as for Y and moderate Ta-Nb depletion (Ionov et al., 2010; Doucet et al., 2012), prevailing for Nb. The REE patterns for peridotitic garnets are mostly round and regular for common peridotite xenoliths. Some of them with S-shaped or even U-shaped REE are typical for the depleted compositions with deep Sr, Zr and Hf troughs as well as for Ba and Th. The levels of Nb, Ta and U, Th fluctuate (Fig. 10A). Ti-rich green garnet from a porphyroclastic wehrlite has very enriched rounded REE pattern but the content of the incompatible elements is very low.

Clinopyroxenes from Zarnitsa reveal rather high REE enrichment and in the patterns which have an inflection in Eu, Ce are more complex and possibly demonstrate the participation of eclogitic material and reactions with peridotites (Fig. 10B). The inclination $(La/Yb)_n$ is moderate. Cpx which are low in REE demonstrate complex S-shaped patterns with very low LREE and strong depletion in Ba. The Cpx compositions with low trace element concentrations also have Zr and Ba minima and low incompatible element abundances. The trace element-rich compositions have higher incompatible element contents but small Ta minima. Garnets from Zarnitsa have commonly rather high LREE except for one harzburgitic sample which shows a minimum in the M-HREE. They show patterns without HFSE minima but strong Ba and Sr depletion, rare U peaks and varying Pb.

For Dalnyaya pipes, the patterns for clinopyroxenes are mainly asymmetric bell-like shapes with a peak at Nd and nearly flat patterns from Ta to Rb with troughs at Ba, Hf and deeper troughs at Zr and Pb. These distributions for the garnets from the concentrates are slightly different from those reported for the xenoliths (Ashchepkov et al., 2016a,b). Garnets mainly show HREE-enriched round patterns, except for one dunitic type, which has low trace elements and S-type REE pattern with a V-shaped depression from

Please cite this article in press as: Ashchepkov, I.V., et al., Alakit and Daldyn kimberlite fields, Siberia, Russia: Two types of mantle sub-terranes beneath central Yakutia?, Geoscience Frontiers (2016), http://dx.doi.org/10.1016/j.gsf.2016.08.004

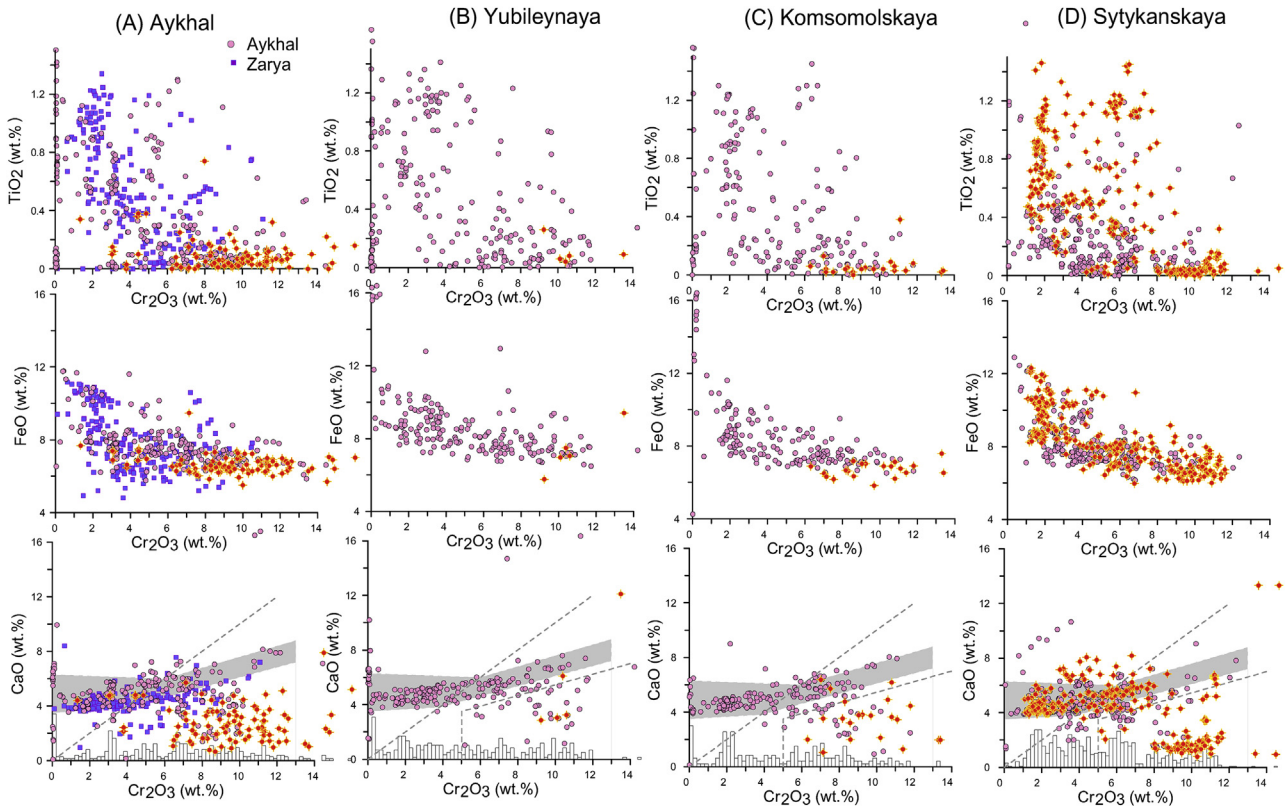

Figure 5. Variation diagrams for mantle clinopyroxenes from the most productive pipes in the Alakit field. (A) Aykhal; (B) Yubileinaya; (C) Komsomolskaya; (D) Sytykanskaya.

Sm to Yb. However, the left part of the spider diagram shows distributions similar to other samples with rather high Ta-Nb and U and low LILE (Fig. 10C).

Clinopyroxenes from the Festivalnaya pipe are very similar to those from Dalnyaya pipe but are more humped in LREE. They show all show Pb peaks and minima and small depressions in Zr and Hf, They reveal also moderated minima in Ta, Nb, Th U and fluctuated LILE. Garnets from this pipe have elevated concentrations and round pattern for the megacrystic pyropes (Fig. 10D). The S-type and depression in the MHREE for harzburgitic patterns are similar to those from the Finsch pipe (Lazarov et al., 2009). The HFSE are near the level of REE. The prevailing REE patterns are tending to be more linear in the middle part than those from Dalnyaya pipe. They demonstrate even enrichment in Nb-Ta and U and depression in Th, U and fluctuating LILE.

6.2. Trace elements in minerals from Alakit field

Four pipes in the Alakit field show distinct features of trace elements of mantle minerals, which differ from those from Daldyn field.

In most productive Aykhal pipe, minerals show rather high enrichment in LREE for both garnets and clinopyroxenes. Cpx shows inclined REE patterns with a small hump at Ce. The Ta, Nb and Zr troughs are correlated with REE levels. Garnets also show different levels of REE and rather gentle slopes compared with garnets from Daldyn field. They show elevated levels of Ta-Nb and even U and Th but the Zr trough is deep for those garnets with low REE concentrations while the Pb peaks are higher (Fig. 11A).

For minerals from the Yubileinaya pipe, LREE enrichment for Cpx is so high that their REE patterns are nearly linear. The patterns with higher $(La/Yb)_n$ inclinations are similar to the high-pressure pyroxenes from Phl-richterite peridotites from Kimberly pipe (Gregoire et al., 2003). Amphibole has concave upward REE and is very similar in trace elements to the composition of one kimberlite from Yubileynaya analyzed also by the LA-ICP-MS method. The garnets vary from S-type patterns which are more common for the Cr-rich garnets to HREE-rich more rounded patterns with and without Ce minima, and even to hampered in the middle part REE pattern common for pyroxenitic garnet (Ashchepkov et al., 2011). Clinopyroxenes show Ti-Pb minima for the most enriched compositions but elevated Th, Nb and U. In contrast, garnets show peaks at Pb and Ti (possibly due to sulfide and ilmenite and micro-inclusions) (Fig. 11B).

Trace elements of minerals from the Komsomolskaya pipe generally show similarities with those from Yubileynaya. Two types of clinopyroxenes demonstrate straight-line REE patterns and different inclinations. The spider diagram has high Th-U and Nb-Ta-Zr minima, less pronounced in Pb. Garnets generally show S-type patterns with low concentrations of all trace elements and a U peak. One garnet shows a round REE pattern and minima in HFSE and Ba (Fig. 11C).

Newly analyzed minerals from the metasomatic veined xenoliths from Sytykanskaya pipe showing higher trace element levels in general and enrichment in LILE, complete the trace element patterns for mantle minerals from this pipe reported previously (Ashchepkov et al., 2013a, 2015). Metasomatic clinopyroxenes show Sr and HFSE at nearly the same levels as REE and sometimes-high Rb due to phlogopite micro-inclusions but a trough in Ba (Fig. 11D).

7. Discussion

In studies by prospecting geologists, the Daldyn-Alakit region is considered as a continuous structure (Ilupin et al., 1990; Khar'kiv et al., 1991; Zinchuk et al., 1993; Zaitsev and Smelov, 2010). There

Please cite this article in press as: Ashchepkov, I.V., et al., Alakit and Daldyn kimberlite fields, Siberia, Russia: Two types of mantle sub-terranes beneath central Yakutia?, Geoscience Frontiers (2016), http://dx.doi.org/10.1016/j.gsf.2016.08.004

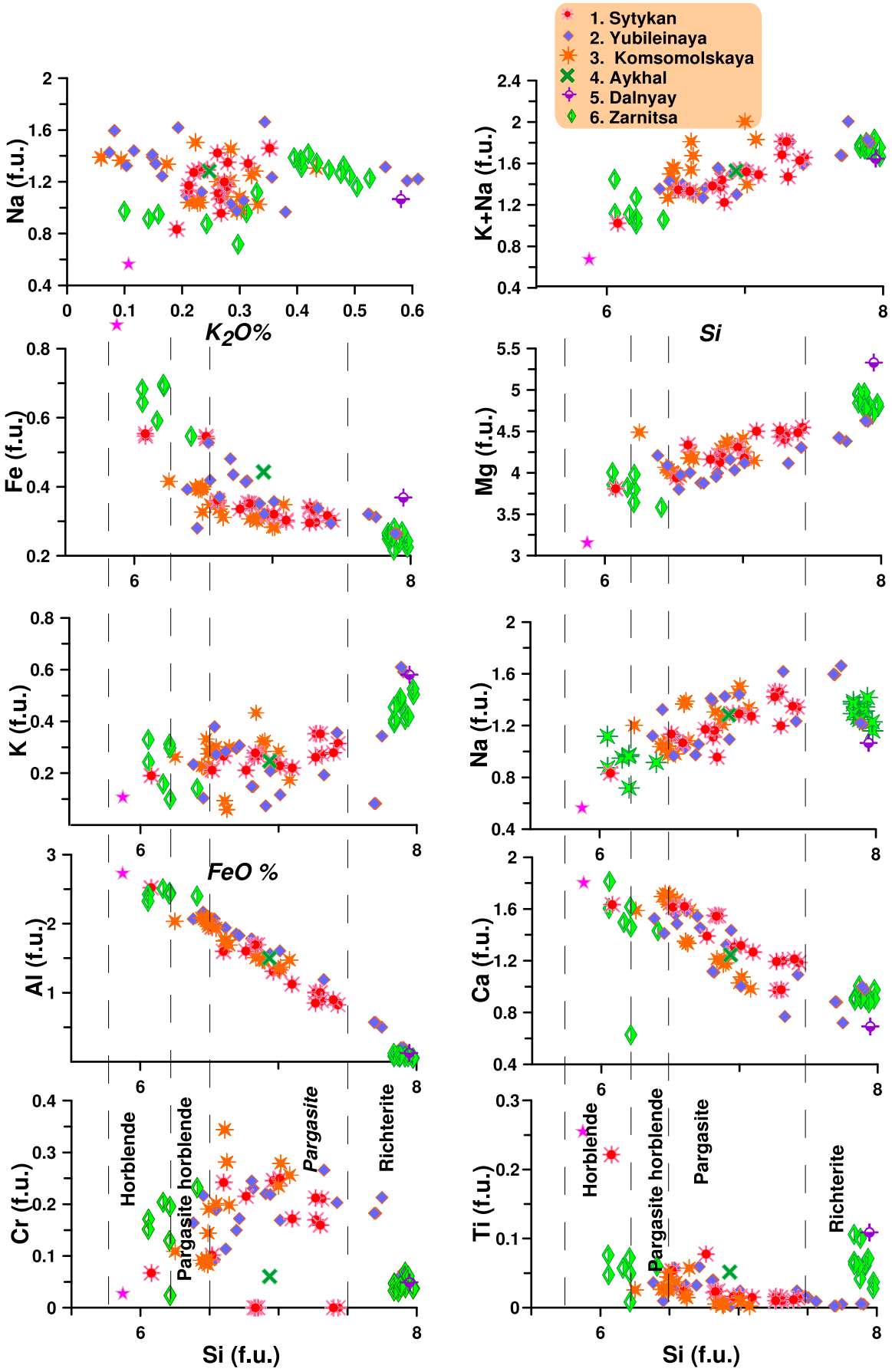

Figure 6. Variation diagrams for mantle amphiboles from the most productive pipes in the Daldyn and Alakit field.

Please cite this article in press as: Ashchepkov, I.V., et al., Alakit and Daldyn kimberlite fields, Siberia, Russia: Two types of mantle sub-terranes beneath central Yakutia?, Geoscience Frontiers (2016), http://dx.doi.org/10.1016/j.gsf.2016.08.004

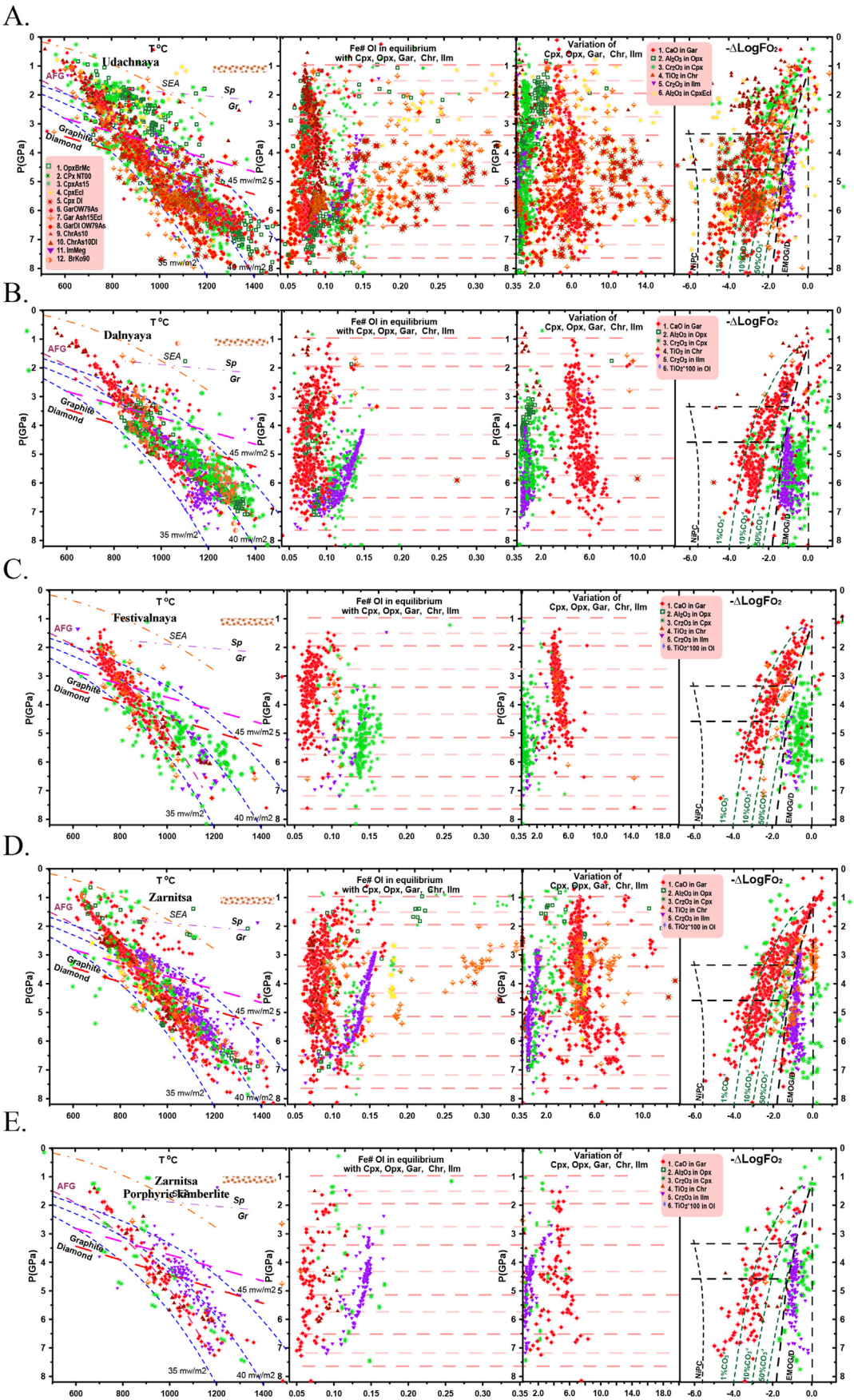

Figure 7. PTXfO_2 diagram for the SCLM beneath Daldyn field. (A) Udachnaya pipe; (B) Dalnyaya; (C) Zarnitsa (ABK); (D) Zarnitsa (PK); (E) Festivalnaya. Symbols: 1. Opx T°C (Brey and Kohler, 1990)- P(GPa) (McGregor, 1974); 2. Cpx: TP (Nimis and Taylor, 2000); 3. T°C (Nimis andTaylor, 2000 cor)- P(GPa)(Ashchepkov et al., 2010); 4. The same for eclogites; 5. The same for diamond inclusions; 6. Gar(mono): T°C (O'Neil and Wood, 1979 mono)-P(GPa) (Ashchepkov et al., 2010); 7. the same for eclogites; 8. The same for diamond inclusions; 9. Chromite: T°C (O'Neil and Wall, 1987)- P(GPa) (Ashchepkov et al., 2010); 10. The same for diamond inclusions; 11. Ilmenite T°C (Taylor et al., 1998)- P(GPa) (Ashchepkov et al., 2010). 12. PT (Brey and Kohler, 1990). The oxidation state was calculated using oxy barometers for Gar (Gudmundsson and Wood, 1995), Ilm, Sp (Taylor et al., 1998) transformed to monomineral equations according to Ashchepkov et al. (2010, 2014a,b). The isopleth of the CO_3^{2-} in melt and position of buffers are according to Stagno et al. (2013).

Please cite this article in press as: Ashchepkov, I.V., et al., Alakit and Daldyn kimberlite fields, Siberia, Russia: Two types of mantle sub-terranes beneath central Yakutia?, Geoscience Frontiers (2016), http://dx.doi.org/10.1016/j.gsf.2016.08.004

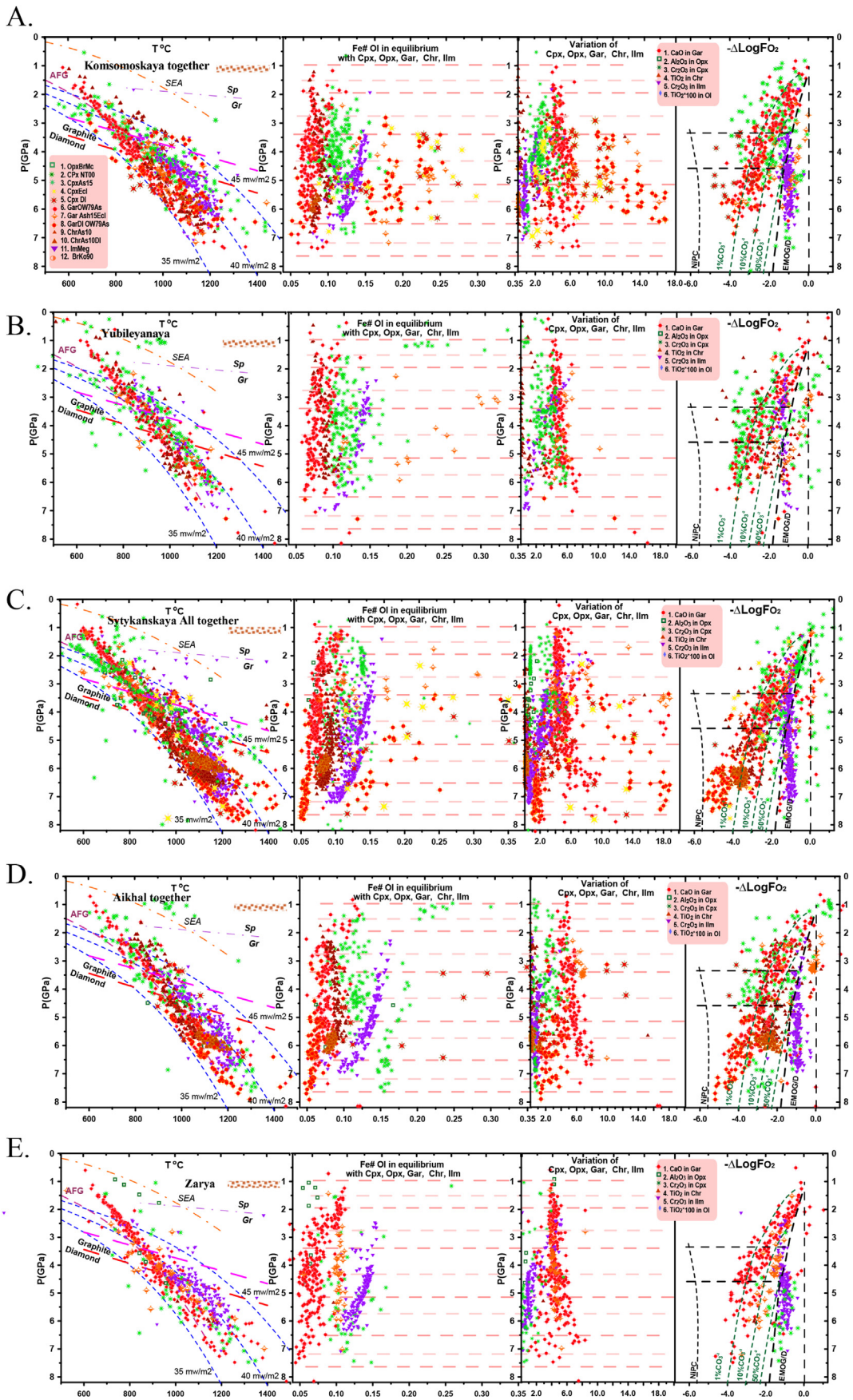

Figure 8. PTXfO_2 diagram for the SCLM beneath Alakit field. (A) Yubileinaya; (B) Komsomolskaya; (C) Sytykanskaya; (D) Aykhal pipe; (E) Zarya pipe. Symbols as for Fig. 7.

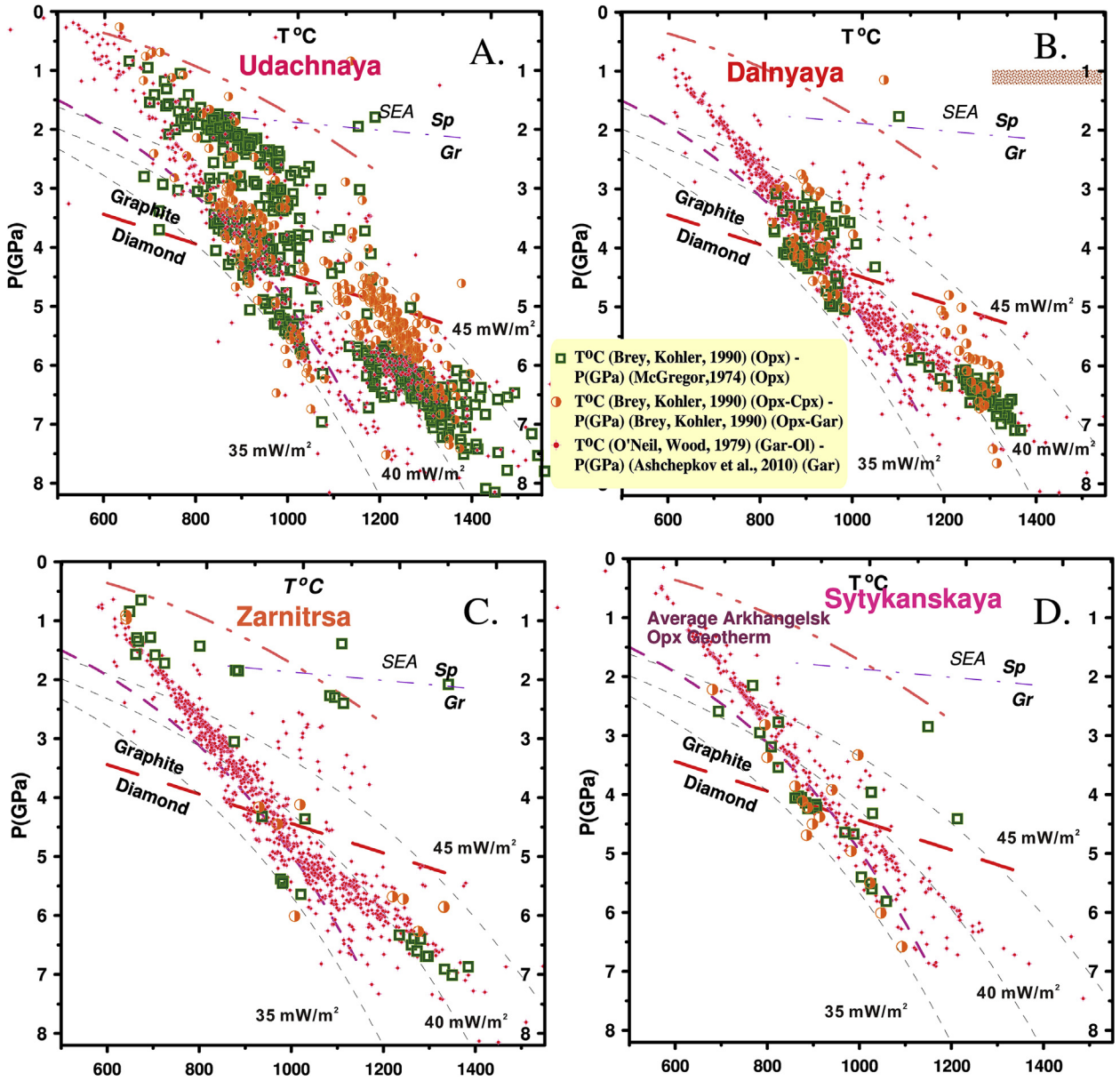

Figure 9. PT diagrams for the SCLM beneath (A) Udachnaya pipe; (B) Dalnyaya; (C) Zarnitsa; (D) Sytykanskaya pipes constructed using the estimates based on Opx and Opx-Gar thermobarometry. Symbols as for Fig. 7.

are no major faults dividing the Daldyn and Alakit fields. However, notable differences and tectonic different positions may suggest that they belong to different sub-terranes. Strong variations in the SCLM structures are notable also in other cratons (Griffin et al., 2004, 2009a,b; Wittig et al., 2008; Zhao et al., 2015) and seen in seismic data (Snyder and Lockhart, 2009; Pedersen et al., 2013).

7.1. Thermobarometric differences of the Alakit and Daldyn fields

More linear geotherms of the Alakit region suggest a uniform growth mechanism of the continental keel and long-term stabilization of the SCLM, whereas the stepped geotherm beneath Daldyn may suggest formation of the mantle keel from alternately hot and cold subducted slabs. This may have happened if they were formed from different subduction slabs originating in distant or proximal spreading centers or formed by fast or slow subduction. The other possibility is that some layers were hydrated to different extents (Doucet et al., 2015; Ivanic et al., 2015). Some layers could be frequent collectors of mantle melts, such as the middle part – the pyroxenite layer (Pokhilenko et al., 1999) or the uppermost SCLM beneath the Moho. The very hot PT arrays shown by the upper part of SCLM beneath Udachnaya and other pipes means a high degree of interaction with the Devonian plume melts penetrating to the Gar-Sp field and underplating beneath the Moho (Thybo and Artemieva, 2013).

The lack of abundant sheared peridotites from the Alakit field may suggest that the deeper layer was not favorable for the intrusion of mantle melts. Possibly it was not weakened by oxidation (Karato, 2010) and/or hydration which is the main reason for shearing (Peslier et al., 2010), whereas the mantle keel beneath Udachnaya was primary hydrated at its base and also in some intermediate levels, which later served as the collector of intruding melts (Doucet et al., 2014).

The other possibility supposes that all terranes were in a back-arc setting and subjected to the influence of arc K-Na melts.

Please cite this article in press as: Ashchepkov, I.V., et al., Alakit and Daldyn kimberlite fields, Siberia, Russia: Two types of mantle sub-terranes beneath central Yakutia?, Geoscience Frontiers (2016), http://dx.doi.org/10.1016/j.gsf.2016.08.004

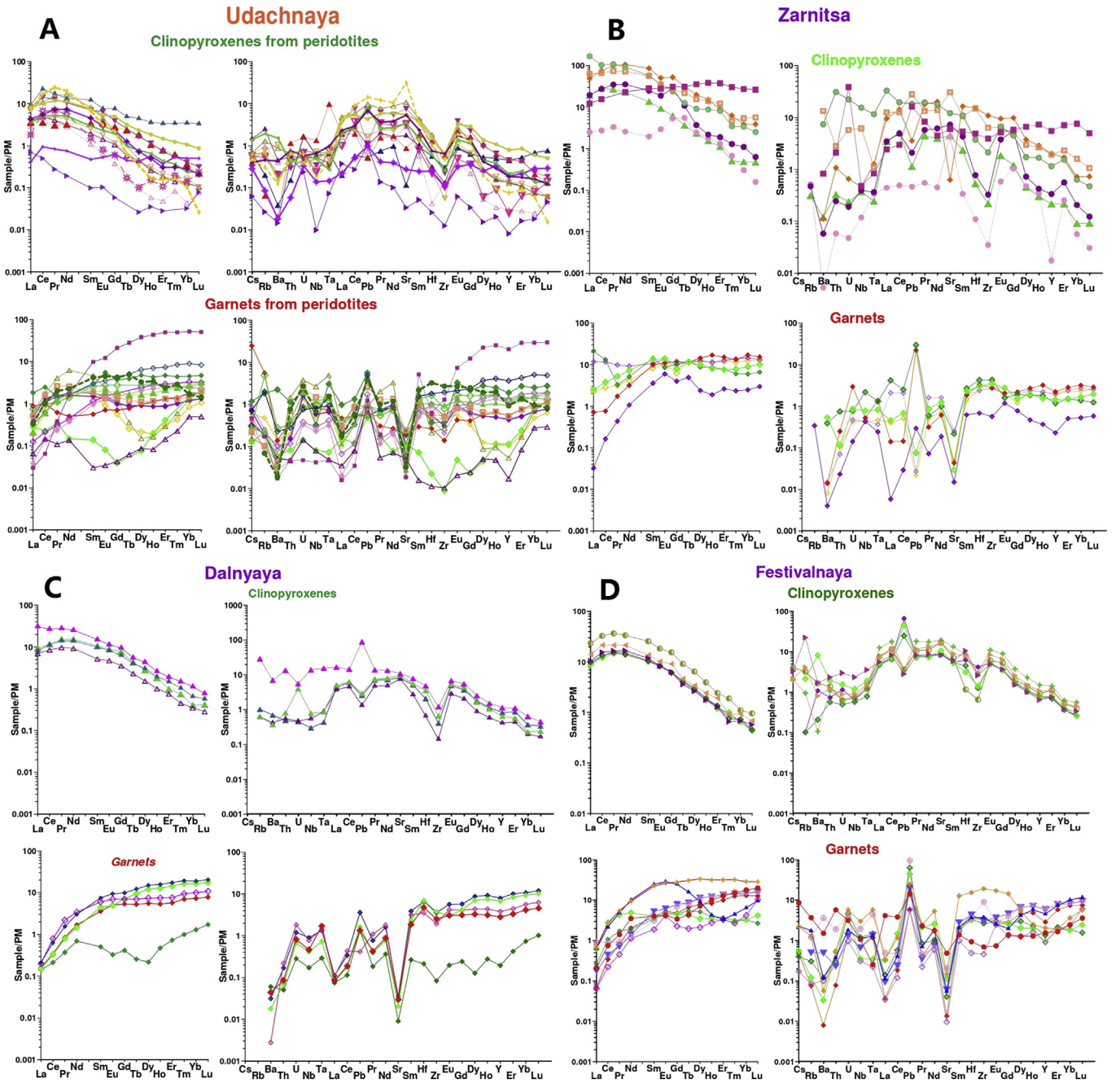

Figure 10. REE and trace element patterns for mantle clinopyroxenes and garnets from Daldyn kimberlite fields. (A) Udachnaya; (B) Zarnitsa; (C) Dalnyaya; (D) Festivalnaya. Normalization to primitive mantle according to McDonough and Sun (1995).

7.2. *Arrays of P-Fe# for garnets*

The question of the formation of the lithospheric keel may be solved using mainly the sequences of P–Fe# for garnets (Ashchepkov et al., 2013a), because pyroxenes are often secondary in peridotites from the SCLM. In the Daldyn SCLM beneath Udachnaya, calculated Fe# for Opx, Gar, Chr and Cpx coexisting with Ol in the peridotite association (Ashchepkov et al., 2010) coincide very well. The details of the P–Fe# for diamond inclusions show that the lithospheric keel in the lower part of SCLM is composed of 7 layers with increasing Fe# with decreasing pressure which is common for oceanic sequences. Rather simple layered structures of the mantle columns are detected in SCLM beneath Udachnaya and Zarnitsa (for PK) pipes in Daldyn field. A general increase in Fe upward suggests that the mantle sequences became more depleted in time in Archean. The opposite inclination corresponds to the interaction of evolved melts with peridotites. Such tendencies are common at the 6.0–6.5 GPa level and correspond to sheared peridotites or other FeG peridotites. In the mantle columns subjected to wide reactions like in SCLM beneath the Zarnitsa (for AKB), Festivalnaya and Dalnyaya pipes, the variations in Fe# are higher and the PT arrays are irregular and together form clouds (Fig. 12).

Beneath Alakit, the Fe#-Ol coexisting with Gar increases continuously or in a stepped manner from the base to the top of the SCLM beneath the large pipes. However, this is stronger for the

Please cite this article in press as: Ashchepkov, I.V., et al., Alakit and Daldyn kimberlite fields, Siberia, Russia: Two types of mantle sub-terranes beneath central Yakutia?, Geoscience Frontiers (2016), http://dx.doi.org/10.1016/j.gsf.2016.08.004

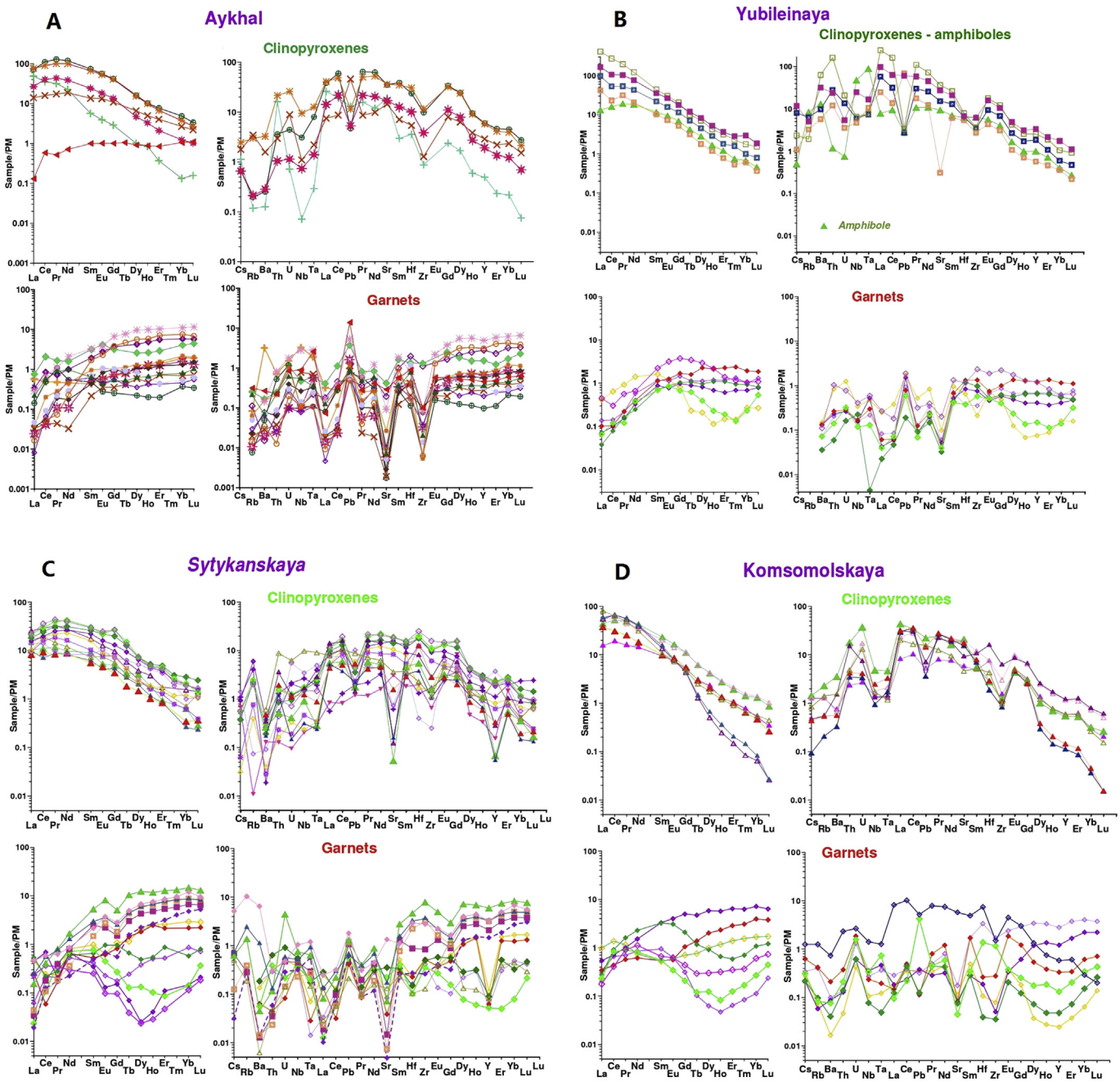

Figure 11. REE and trace element patterns for mantle clinopyroxenes and garnets from Alakit kimberlite field. (A) Aykhal; (B) Yubileinaya; (C) Sytykanskaya; (D) Komsomolskaya. Normalization to primitive mantle according to McDonough and Sun (1995).

SCLM beneath the Aykhal pipe. In the Sytykanskaya SCLM, the reactions show three arrays from 5.5 to 3 GPa. For the SCLM beneath the Yubileynaya and Komsomolskaya pipes, the general growth from the lithosphere base to the middle SCLM is observed but the variations in $Fe^{\#}$ are higher. The common tendency is that the simpler and rough layering like in Aykhal and Udachnaya pipes coincides with higher diamond grades.

An example of the evolution of the mantle column beneath Zarnitsa from simple layering sampled by the early PK kimberlites to more complex arrays determined for AKB, or from Aykhal to Zarya SCLM, show that large metasomatic perturbation reduces the diamond grade.

Some difference in the layering in the Alakit SCLM from Aykhal to Sytykanskaya (East Daldyn terrane) determined by garnets suggests lateral variations, for example domination of dunitic associations near the lithosphere base beneath Sytykanskaya pipe. Nevertheless, one could also see the similarities not only within one field but in all regions from Krasnopresnenskaya to Udachnaya (Fig. 14).

7.3. General regularities of the mantle patterns for minerals as evidence of mantle processes

High variations of mantle mineral REE and patterns and spider diagrams for some pipes such as Udachnaya, Sytykanskaya and

Please cite this article in press as: Ashchepkov, I.V., et al., Alakit and Daldyn kimberlite fields, Siberia, Russia: Two types of mantle sub-terranes beneath central Yakutia?, Geoscience Frontiers (2016), http://dx.doi.org/10.1016/j.gsf.2016.08.004

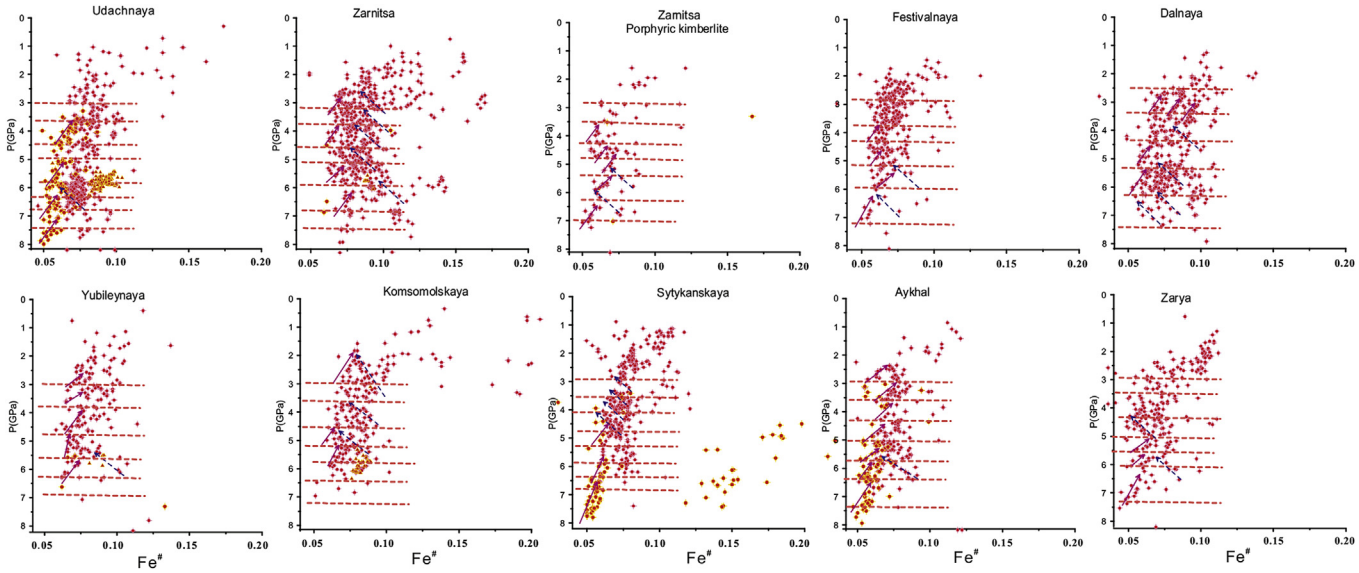

Figure 12. P–Fe# for the garnets from SCLM beneath the large productive kimberlite pipes in Daldyn and Alakit fields.

Dalnyaya were already discussed (Ashchepkov et al., 2013a,b, 2015, 2016a,b). Comparison shows that variations of the patterns of Cpx from Udachnaya and Zarnitsa in the Daldyn field are higher than for the Cpx from Aykhal and Komsomolskaya pipes. Also, the V-shaped dunitic patterns (Banas et al., 2009) are more frequent in the Daldyn field while harzburgites with HREE depression are common for the Alakit SCLM. The depth of the HREE is likely regulated by the Gar/Cpx ratios and degree of melting as well as intensity of chromatographic melt percolation effects (Harte et al., 1993; Doucet et al., 2012). The S-type patterns for garnet are very common for the pipes in the Alakit field possibly demonstrating pronounced melt percolation effects (DePaolo, 1981). Some round depressions of the garnets and clinopyroxenes from the Alakit region, as well as the general depletion of rocks, are similar to the peridotites from back-arc or even fore-arc settings (Ionov et al., 2013). However, it is not easy to suggest why and how back-arc peridotites were merged to the craton keel and why the mantle rocks at distances of <100 km have moderate depletion and MORB-type characteristics.

Subduction related characteristics such as Sr, U, Ba, Pb peaks and HFSE depression (Spandler et al., 2004) are very rarely detected for trace element patterns of mantle minerals from both the Daldyn and Alakit fields. This suggests that subduction conditions differed in Archean times (Shu and Brey, 2015). Possibly also, most mantle rocks were subjected to later melt interaction and to metasomatism.

7.4. Metasomatic agents

Several types of mantle metasomatism are described for mantle rocks (Harte et al., 1993; Griffin et al., 1999b; McCammon et al., 2001; Gregoire et al., 2003; Araújo et al., 2009; Banas et al., 2009; Nimis et al., 2009; Pokhilenko et al., 2013; Agashev et al., 2013; Doucet et al., 2014; Shu and Brey, 2015; Le Roex and Class, 2016). But major differences lie in the nature of the agents: H_2O bearing or carbonatitic melts or fluids. The results of metasomatism also depend on the oxidation state (Hanger et al., 2015).

Abundant hydrous metasomatism in the mantle of the Alakit field is pronounced not only in the Stykanskaya pipe (Ashchepkov et al., 2015), where amphiboles and phlogopites occur in veins and are scattered in the peridotites. They are also common in xenoliths of all other large pipes. The multistage metasomatism rich in the LILE and other trace elements may suggest that this part of the mantle lithosphere was located at the margin of the craton, and possibly was subjected to the influence of subduction-related mantle fluids (Ma et al., 2016) derived from the mica-bearing sediments, which can produce huge Rb-Ba, anomalies or even subducted proto continental TTG crust (Halla et al., 2009). Ancient (hydrous) metasomatism rarely could be associated with Zr, Hf, Y growth as for the Belsbank peridotites (Shu and Brey, 2015).

In metasomatic associations formed by H_2O-bearing melts, chromites dominate over ilmenites typical for mantle veins beneath the Daldyn field (Dalnyaya and Festivalnaya), which are associated with carbonatitic (Chakhmouradian, 2010) or protokimberlite melts which produced the enrichment in HFSE. Such Nb-Ta enrichment is common for mantle associations from the Dalnyaya (Ashchepkov et al., 2016a,b) and Festivalnaya pipes. The carbonatites which are not related to magmas produced U-Th enrichment which is very rare for minerals from the SCLM. Highly oxidized melts could produce huge HFSE negative anomalies (Ashchepkov et al., 2014b).

Rather high Fe and sometimes Ti in metasomatic veins in Alakit SCLM is also evidence of the influence of evolved melts of possibly of hybrid H_2O-carbonatite nature related to ancient plumes (Ashchepkov et al., 2015) or later protokimberlites.

7.5. Trace element evidences for the mantle processes and reconstructions

7.5.1. Equilibrium – disequilibrium features for Gar-Cpx bearing melts and the stages of melts percolation

Here we compare mainly peridotitic garnets and clinopyroxenes, because melts in equilibrium with the megacryst as for Cpx from Dalnyaya show features close to protokimberlite (Ashchepkov et al., 2016a,b).

The comparison of the melts parental for the minerals (PMM) determined using KD of mineral/melts for Gar (Green et al., 2000) and Cpx (Hart and Dunn, 1993) shows that PMM responsible for the creation of garnets (Fig. 8) and clinopyroxenes differ in their configurations of spider diagrams. The PMM patterns for the clinopyroxenes are often more enriched in trace elements (Fig. 13). The difference in configurations reflects the fact that pyroxene peridotite associations were created later and, in many cases from the

more evolved or low degree partial melts (LDM). However, garnets in many cases were formed during construction of the lithospheric keel from melts of higher degree of fusion or differing in volatile content. Garnet formation mainly occurred close to the main merging events of the late Archean collision (Malkovets et al., 2012).

The PMM for Cpx in both Alakit and Daldyn SCLM show more flatter patterns and the PMM for garnets reveal some round depression in the HREE (Ashchepkov et al., 2013b), likely reflecting the chromatographic effects of melt percolation in the garnet stability field (Harte et al., 1993).

The clinopyroxenes are located in intergranular positions in the rocks or form microveins. In most cases, they reflect the later events of melt percolation through the mantle columns. Clinopyroxenes commonly show Pb-troughs due to the precipitation of sulfides, which accompanied differentiation, whereas garnets show Pb peaks probably common for partial melting when intergranular sulfides participate in melt generation. The U peaks found in garnet spider grams results from interaction with subduction-related fluids.

The difference is in the elevation of REE level relative to primitive mantle (PM) (McDonough and Sun, 1995), and mainly corresponds to depletion in modal melting events. However, it also reflects the melting degrees (F) and abundance of the remaining garnets in the rocks (Rollinson, 1993) in the melting events corresponding to hydrous melting. Abundance of olivine could even raise the REE level as well as Gar/Cpx ratio in the restite. Rocks that are depleted in Cpx rocks produce more inclined and LREE enriched patterns.

Thus, the high REE content and inclination for the PMM for Cpx from Alakit in many cases indicates their formation during metasomatism from hydrous or carbonatite low degree partial melts (Frezzotti and Touret, 2014). Trace element patterns of the Alakit garnets in many cases may characterize primary ancient features, though there are many Ti-bearing varieties, which obtained their secondary characteristics under the influence of plume-derived or other metasomatic melts. The amount of garnets showing HREE-depletion is higher in the Alakit pipes than in Udachnaya and other kimberlite pipes from the Daldyn field.

Alakit garnets commonly have no deep Y minima. The extraction of this element which is compatible for garnet ($KD_{Y\ in\ Gar} = 3.5–14$) (Green et al., 2000; Bédard, 2006) may be explained just by removal of garnet from the rock. It may also be explained by the removal of zircons or Y-phosphates producing deeper anomalies. Commonly spinel peridotites have no Y anomalies, but special metasomatism with formation of zircons found in island arcs or participation of P-rich fluids could create such anomalies. The garnets from Daldyn often demonstrate rather flat HREE patterns and thus garnet extraction is under question.

Daldyn minerals reveal frequent Y anomalies, suggesting essential melting in garnet stability field. The high variation in Zr,

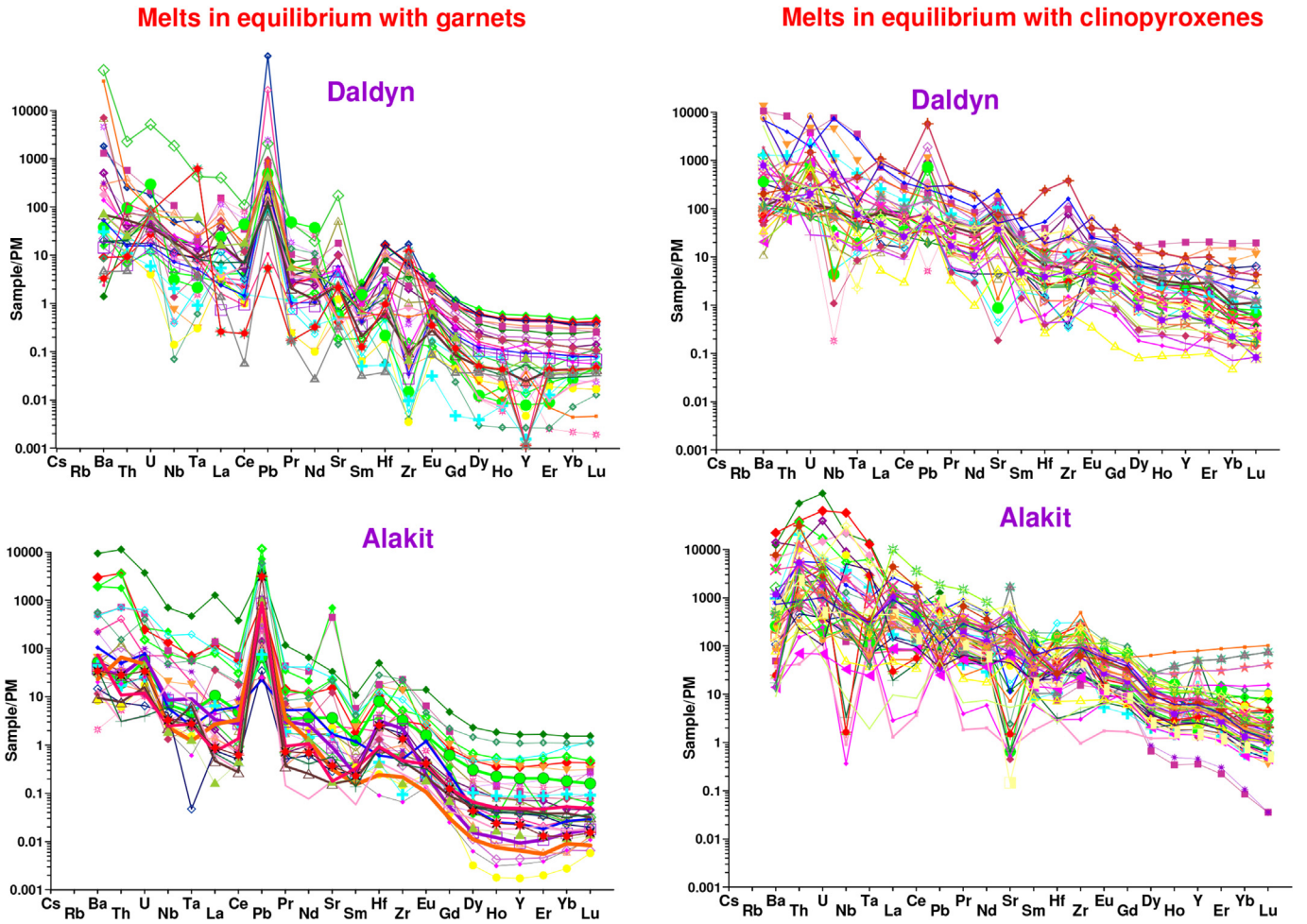

Figure 13. REE and trace element diagrams for melts parental for mantle garnets and clinopyroxenes from Daldyn and Alakit kimberlitic fields, Siberian platform. Normalization to primitive mantle according to McDonough and Sun (1995).

Please cite this article in press as: Ashchepkov, I.V., et al., Alakit and Daldyn kimberlite fields, Siberia, Russia: Two types of mantle sub-terranes beneath central Yakutia?, Geoscience Frontiers (2016), http://dx.doi.org/10.1016/j.gsf.2016.08.004

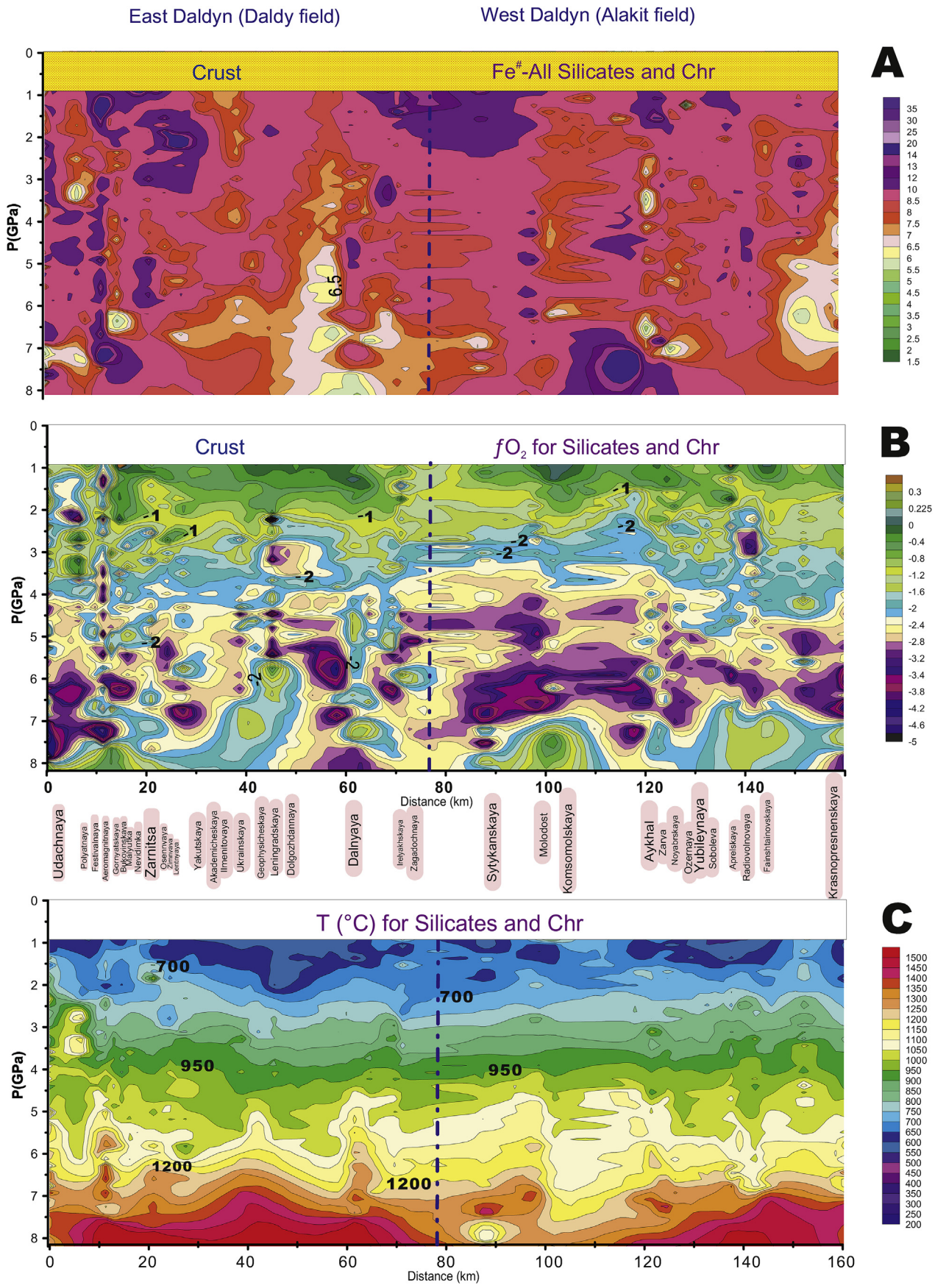

Figure 14. Schematic SCLMT through Daldyn field (contour maps) from Udachnaya to Zagadochnaya pipe based on: (A) P–Fe# for all minerals; (B) P–fO_2 for all minerals; (C) P–T.

Please cite this article in press as: Ashchepkov, I.V., et al., Alakit and Daldyn kimberlite fields, Siberia, Russia: Two types of mantle sub-terranes beneath central Yakutia?, Geoscience Frontiers (2016), http://dx.doi.org/10.1016/j.gsf.2016.08.004

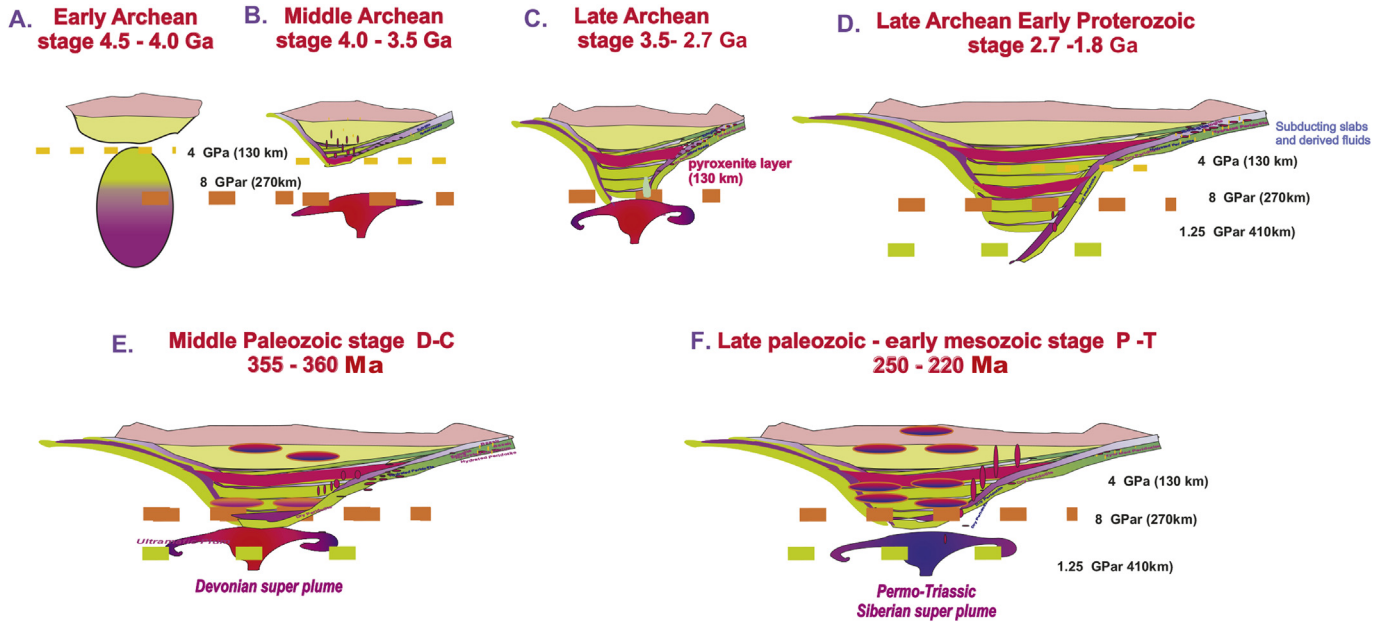

Figure 15. Scheme of the growth and development of mantle keel beneath Siberian Craton. (A) Early Archean stage. Highly differentiated mantle diapir and separation crust and depleted mantle; (B) middle Archean stage. Creation of proto continent shallow subduction with melting of eclogites; the pyroxenite layer 120–150 km; (C) late Archean stage. Low angle subduction with the spalling of the slabs beneath the continents; (D) late Archean–early Proterozoic stage. Creation of the protocontinents with the super thick mantle lithosphere; (E) middle Paleozoic Devonian stage. Interaction of the Devonian superplume with the continents with the creation of basalt in rifting area and kimberlites ion rift shoulders; (F) late Paleozoic–early Mesozoic stage. Interaction of Siberian Superplume with Siberian continent. Rifting creation of basalts and kimberlites.

Hf and Ta-Nb troughs is also more common for the parental melts for the garnets from this field.

Our wider range of trace element data for minerals from Udachnaya pipe was recently described (Ashchepkov et al., 2012, 2013a,b). Trace elements of this suite are most variable. There are many inflected patterns reflecting the wide variations in mantle rock compositions.

For the Cpx from Alakit pipes, the high inclination of REE patterns and LREE-enrichment is typical for PMM from all pipes but notable differences occur between the northern pipes Sytykanskaya and Komsomolskaya, including the Yubileynaya and Aykhal pipes. Many of them have high LILE content. Rb anomalies for Cpx from Sytykanskaya commonly are associated with Phl metasomatism.

The PM or pyroxenes from the Sytykanskaya pipe from xenoliths without phlogopites are slightly less LREE-enriched and humped with a peak at Pr showing in spider diagrams and Zr, Pb minima, Th maximum and varying Nb-Ta. Cpx from Sytykanskaya and Komsomolskaya show troughs at Zr-Hf and Zr, but the latter component varies in Cpx from Yubileynaya. The Zr trough in CPx from the Komsomolskaya pipe and decoupled Hf probably relate to H_2O metasomatism (Griffin et al., 1999a). The Zr troughs, which are typical for Phl metasomatism, are also common for parental melts from Zarnitsa pipe (Griffin et al., 1993, 1999a; Downes et al., 2015).

7.6. Possible geomechanics of the mantle keel growth and destruction beneath Siberian craton

The structure of the SCLM, geochemical characteristics of the mantle minerals and parental melts, as well as bulk rock compositions (Boyd et al., 1997; Ionov et al., 2010; Doucet et al., 2012) may be used as the basis of the reconstructions of paleodynamic environments.

In the Daldyn SCLM (East Daldyn terrane), bulk rock compositions and geochemistry of melts parental for minerals suggest that it was composed from primary oceanic peridotites (Ionov et al., 2010; Doucet et al., 2012; Goncharov et al., 2012; Ashchepkov et al., 2013b), formed probably in the middle–late Archean (Pearson et al., 2005; Malkovets et al., 2012) and reactivated in late Proterozoic (Ionov et al., 2015) during collision events (Rosen et al., 2005, 2006).

To suggest an arc origin of the highly depleted peridotites from Alakit (and other regions), it is necessary to prove the fact of subduction of fore- or back-arc peridotites together with the arc itself and probably the sediments from the ancient TTG (Halla et al., 2009), which could be the source of the Fe-rich high-Al eclogites (Spetsius et al., 2008; Riches et al., 2010). The high-Mg and Cr-low eclogites, which are common in Alakit (Pernet-Fisher et al., 2014), are complemental to TTG (Horodyskyj et al., 2007).

The detailed structure showing variations of $Fe^{\#}$ of peridotitic garnets suggests that the lower part of the SCLM was composed of several (6–7) paleo subduction slabs.

The high depletion of peridotites, abundant hydrous metasomatism with higher participation of the LILE (Aykhal pipe) and other incompatible elements in geochemistry of parental melts, may mean a continental or even back-arc environment of peridotite formation. The mantle wedge (Ntaflos et al., 2007) in present time is more depleted that it should be in Archean time due to lower water activity. Extended P–$Fe^{\#}$ Cpx arrays suggests large-scale melt percolation and metasomatism.

The high alkalinity of clinopyroxenes from the Alakit region could be explained by several possible mechanisms. One is transformation of peridotites hydrated by marine water. Next is metasomatic interactions with subduction-related fluids in the marginal cratonic setting. Another reason that is more probable is interaction of the melted subducted basalts (spilites) transformed later to eclogites and peridotites.

The structure of the Daldyn Alakit region shown on the mantle lithosphere profile (Fig. 14) obtained by the method described previously (Ashchepkov et al., 2014a,b) shows that it is slightly folded but shows rather continuous structure, which suggests that

Please cite this article in press as: Ashchepkov, I.V., et al., Alakit and Daldyn kimberlite fields, Siberia, Russia: Two types of mantle sub-terranes beneath central Yakutia?, Geoscience Frontiers (2016), http://dx.doi.org/10.1016/j.gsf.2016.08.004

this part of the mantle keel was formed in the same stage and possibly represents the same structure, but with lateral changes in composition of the constituting rocks (Fig. 14). However, one could see that between Zagadochnaya to Sytykanskaya, the structure of layering slightly changes and the lower part of the mantle section becomes more depleted. It is possible that Daldyn and Alakit could represent closely located but separate blocks combined in one terrane in very ancient time.

The seismic data and modeling of profiles in the Siberian craton SCLM (Kuskov et al., 2011; Pavlenkova, 2011) give in general the same thickness of the lithosphere and even the amount of layers but the resolution is rather low.

7.6.1. Stages of the SCLM growth

Possible mechanisms of the creation and evolution of the craton keel were described in many publications (Griffin and O'Reilly, 2007; Pearson et al., 2005; Santosh et al., 2009; Santosh, 2010; Lee et al., 2011; Griffin et al., 2014). In the early stage, the most probable mechanism is a deep mantle diapir or slow plume with high melting degrees in heated early Archean mantle (Aulbach, 2012) (Fig. 15A). Such depleted cores of the ancient cratons are recognized in Zimbabwe (Smith et al., 2009), in the North Atlantic craton (Wittig et al., 2008; Sand et al., 2009) and probably in Aldan shield. However, the layered structures, which are detected beneath most continents, may be created only because of subduction (Pearson, 1999; Pearson et al., 2005). Thus, in the stages around 4.0 or 4.4 billion years a magma ocean corresponds to the highly depleted spinel peridotites. In the early stages with a hot mantle, the thickness of the keel was about 120 km (van Hunen and van den Berg, 2008). The eclogitization at that time took place only to the depth of 120 km. In deeper conditions, eclogites should melt due to the high temperatures and oxidized conditions of the slab in HT conditions of the Archean mantle (Fig. 11B). Eclogites transformed to pyroxenites show a range of compositions consistent with their arc origin (Horodyskyj et al., 2007). The thickness of mantle created at the stages of the intra-oceanic arcs (Maruyama et al., 2012) corresponds to Ga-Sp peridotites of the upper part of mantle. The pyroxenite-eclogite layers at the depth of 3.5–4.0 GPa represent the enriched bottom of the keels created by the re-melted eclogites, and variations from 3 to 4 GPa probably relate to the different time of creation of this boundary.

The very cold ledge at ~3 GPa to 600 °C found for the SCLM of Udachnaya and some other pipes probably reflects the conditions of deep melting and fast subduction at the beginning of the process of the fast SCLM growth after 3.0–2.7 billion years, which probably relates to the time period of the small embryonic protocontinents (Maruyama et al., 2012; Roberts et al., 2015), when after a small amount of cooling subducted slabs cannot cross the 8.0 GPa boundary of the olivine melt density inversion (Agee, 1998) (Fig. 11C). The thermal conditions were hot enough for melting of most eclogites and creation of the pyroxenite layers in different parts of the lower SCLM and lithosphere base (Ashchepkov et al., 2010, 2011, 2013a,b) beneath Udachnaya, Mir and other large pipes. During the general cooling of the Earth's mantle (Gerya, 2014), the eclogite layers could be subducted to the upper-lower mantle transition zone. After transformation they may fall into the lower mantle and after melting create plumes (Maruyama and Okamoto, 2007).

The question of how >100 km of lower SCLM with similar characteristics in their peridotites can be created is debatable. They may be easily created by the stacking of the inclined subduction slabs (Gerya, 2014; Griffin et al., 2014; Humphreys et al., 2015), but the SCLM reconstructions suggested the relatively uniform structures beneath the same kimberlite region like in the Daldyn terrane relates to the model of low angle subduction (Snyder and Lockhart, 2009). Similar structures with the low angle rhythmic layering were determined by seismic methods for the Slave (Snyder and Lockhart, 2009) and other cratons. The common division of the SCLM to large 6 (or 12 units) (Ashchepkov et al., 2010, 2014a,b) may be determined by the common thickness of the subducting slabs close to 20 km which together combine to form the 200–250 km^2 of the SCLM. According to isotopic data, the growth of SCLM should be accomplished by 2.7 Ga, coinciding with the peaks of crustal global growth (Kröner et al., 2012; Roberts and Spencer, 2015), creation of supercontinent Sclavia (Nance et al., 2014) and creation of garnets in mantle peridotites (Malkovets et al., 2012) and appearance of water in mantle (Santosh et al., 2009).

The period of the SCLM accretion of large continents was finished near 2.3–1.8 billion years, with the appearance of the first supercontinent Protopangea (Piper, 2010) or Columbia (Nuna) (Santosh et al., 2009; Maruyama et al., 2012). This event is well detected by Re-Os isotopes for Siberian mantle (Ionov et al., 2015). It was the stage of the abundant hydrous subduction-related metasomatism (Pokhilenko et al., 2013). Probably at this stage, the continental lithosphere thickness could have reached 330 km, and in some cases maybe 410 km (O'Reilly et al., 2009) in cold conditions with fast subduction, at least beneath intracontinental collision zones (Fig. 15D) and when the convection beneath the continents stopped. At that time, the thermal gradient could be near 33 mW/m^2 or less (Artemieva, 2009) while the continental thickness of 250–270 km relates to the 38–40 mW/m^2 geotherm (Rudnick et al., 1998). It is a question whether some remnants of such deep roots still exist (O'Reilly et al., 2009; O'Reilly and Griffin, 2010). Probably they were in Siberia to the time of kimberlite intrusion, because pyrope garnets with up to 16 wt.% Cr_2O_3 occur in the lithosphere.

In the Proterozoic, the history of the continental keel growth finished. Break-up of the supercontinents after a series of superplumes and the creation of Rodinia amalgamated Siberia. The latest significant modifications refer to 1.8 Ga (Ionov et al., 2015). The further history was mainly destruction and rifting. Daldyn mantle contains phlogopites crated mainly in Proterozoic time (Pokhilenko et al., 2013) while Alakit mantle phlogopites are Neoproterozoic–Phanerozoic (Ashchepkov et al., 2015) (Supplementary file 2).

Continuous oxidation of Earth mantle and melts was accompanied by the appearance of the melt lenses in the SCLM at 6.0 GPa at the minimum of the oxidation solidus of peridotites (Foley, 2011). This was accompanied by reduction of lithosphere thickness to 250 km in late Proterozoic and Paleozoic, and especially in Mesozoic time, though deeper roots are also recognized (Fishwick, 2010; O'Reilly and Griffin, 2010).

After the Permo–Triassic plumes, the presence of deep roots >200 km are not evident by the P–T estimates based on the mineral concentrates from most northern kimberlite fields, as well as from geophysical models (McKenzie and Priestley, 2008; Koulakov and Bushenkova, 2010; Kuskov et al., 2011; Pavlenkova, 2011). Garnets, pyroxenes and some xenoliths captured from the level of 6.0 GPa in Kharamai and other Triassic kimberlite fields (Griffin et al., 2005; Ashchepkov et al., 2016a) are common in the Triassic kimberlites. It is possible that basification and thermomechanical interaction of a superplume with the SCLM reduced the thickness of the lithosphere in 30–50 km, as was calculated by Sobolev et al. (2011).

7.6.2. Nature of differences in SCLM between Alakit and Daldyn field

The primary difference in the mineral geochemistry could possibly be explained by the different origin of these terranes or their different positions in the structure of the continent. The latter

Please cite this article in press as: Ashchepkov, I.V., et al., Alakit and Daldyn kimberlite fields, Siberia, Russia: Two types of mantle sub-terranes beneath central Yakutia?, Geoscience Frontiers (2016), http://dx.doi.org/10.1016/j.gsf.2016.08.004

is more probable because the profiles for the Daldyn and Alakit show that the mantle structure is nearly continuous.

It is possible that the West Daldyn terrane was in ancient time at the margin of the continent and was subjected to hydrous melting with many stages of melt intrusion activated by subduction of evolved sediments abundant in mica. This also could explain the relatively cold geotherm and linear shape, because metasomatism produced homogenization of the mantle column, although the garnets still keep the signs of primary mantle layering.

8. Conclusions

(1) Systematic differences were found in the chemistry and trace element patterns of mantle minerals found as xenoliths and xenocrysts from the kimberlites of Alakit (more enriched and metasomatized) and Daldyn region (more depleted).
(2) The differences in the mineralogy most likely reflect the tectonic positions of the mantle terrains. The Alakit field in the West Daldyn terrain relates to the marginal part of craton subjected to subduction metasomatism.
(3) Despite the general similarities in the SCLM structures within the same kimberlite, mantle columns are not similar and even pipes could have rather different structure and diamond grades.
(4) Mantle columns subjected to a high degree of metasomatism or melt interaction such as those beneath the Dalnyaya and Zarnitsa pipes show dispersed clouds in the PT diagrams and P–$Fe^{\#}$ trends.
(5) The pipes with the preserved primary layering of the SCLM and low dispersion like Aykhal or Udachnaya have higher diamond grades.
(6) Early Archean subducted slabs melted at 130–150 km creating pyroxenite layer.
(7) Creation of SCLM structure was accomplished 3.0–2.5 Ga with the appearance of H_2O in mantle with the latest modification 1.8–2.0 Ga and later metasomism in the Daldyn 2.4–0.7 Ga and in the Alakit SCLM from 1.8 to 0.5 Ga

Acknowledgements

Supported by Grants RBRF 05-05-64718, 03-05-64146; 11-05-00060a; 11-05-91060-PICSa; 16-05-860. The work contains the result of the projects 77-2, 65-03, 02-05 UIGGM SD RAS and ALROSA Stock Company. We grateful Austrian Academy of Sciences invited I.V. Ashchepkov to Vienna University for study of Siberian xenoliths. We are grateful to ALROSA Company for the samples and kimberlite concentrates. We are grateful also to Associate Editor, Dr. Nick Roberts for the improvements on the text.

Appendix A. Supplementary data

Supplementary data related to this article can be found at http://dx.doi.org/10.1016/j.gsf.2016.08.004.

References

Agashev, A.M., Ionov, D.A., Pokhilenko, N.P., Golovin, A.V., Cherepanova, Y., Sharygin, I.S., 2013. Metasomatism in lithospheric mantle roots: constraints from whole-rock and mineral chemical composition of deformed peridotite xenoliths from kimberlite pipe Udachnaya. Lithos 160–161, 201–215.

Agashev, A.M., Pokhilenko, N.P., Tolstov, A.V., Polyanichko, N.P., Mal'kovets, V.G., Sobolev, N.V., 2004. New data on age of kimberlites from Yakutian kimberlite province. Doklady Earth Sciences RAN 399, 95–99.

Agee, C.B., 1998. Crystal-liquid density inversions in terrestrial and lunar magmas. Physics of the Earth and Planet Interiors 107, 63–74.

Alifirova, T.A., Pokhilenko, L.N., Korsakov, A.V., 2015. Apatite, SiO_2, rutile and orthopyroxene precipitates in minerals of eclogite xenoliths from Yakutian kimberlites, Russia. Lithos 226, 31–49.

Artemieva, I.M., 2009. The continental lithosphere: reconciling thermal, seismic, and petrologic data. Lithos 23-46, 2009.

Araújo, D.P., Griffin, W.L., O'Reilly, S.Y., 2009. Mantle melts, metasomatism and diamond formation: insights from melt inclusions in xenoliths from Diavik, Slave Craton. Lithos 112 (2), 675–682.

Ashchepkov, I.V., Vladykin, N.V., Nikolaeva, I.V., Palessky, S.V., Logvinova, A.M., Saprykin, A.I., Khmel'nikova, O.S., Anoshin, G.N., 2004. Mineralogy and geochemistry of mantle inclusions and mantle column structure of the Yubileinaya Kimberlite Pipe, Alakit Field, Yakutia. Doklady of RAS ESS 395 (4), 517–523.

Ashchepkov, I.V., Pokhilenko, N.P., Vladykin, N.V., Logvinova, A.M., Kostrovitsky, S.I., Afanasiev, V.P., Pokhilenko, L.N., Kuligin, S.S., Malygina, L.V., Alymova, N.V., Khmelnikova, O.S., Palessky, S.V., Nikolaeva, I.V., Karpenko, M.A., Stagnitsky, Y.B., 2010. Structure and evolution of the lithospheric mantle beneath Siberian craton, thermobarometric study. Tectonophysics 485, 17–41.

Ashchepkov, I.V., Andre, L., Downes, H., Belyatsky, B.A., 2011. Pyroxenites and megacrysts from Vitim picrite-basalts (Russia): polybaric fractionation of rising melts in the mantle? Journal of Asian Earth Sciences 42, 14–37.

Ashchepkov, I.V., Rotman, A.Y., Somov, S.V., Afanasiev, V.P., Downes, H., Logvinova, A.M., Nossyko, S., Shimupi, J., Palessky, S.V., Khmelnikova, O.S., Vladykin, N.V., 2012. Composition and thermal structure of the lithospheric mantle beneath kimberlite pipes from the Catoca cluster, Angola. Tectonophysics 530–531, 128–151.

Ashchepkov, I.V., Vladykin, N.V., Ntaflos, T., Downes, H., Mitchell, R., Smelov, A.P., Alymova, N.V., Kostrovitsky, S.I., Rotman, A.Ya, Smarov, G.P., Makovchuk, I.V., Stegnitsky, Yu.B., Nigmatulina, E.N., Khmelnikova, O.S., 2013a. Regularities and mechanism of formation of the mantle lithosphere structure beneath the Siberian Craton in comparison with other cratons. Gondwana Research 23, 4–24.

Ashchepkov, I.V., Ntaflos, T., Kuligin, S.S., Malygina, E.V., Agashev, A.M., Logvinova, A.M., Mityukhin, S.I., Alymova, N.V., Vladykin, N.V., Palessky, S.V., Khmelnikova, O.S., 2013b. Deep-seated xenoliths from the brown breccia of the Udachnaya pipe, Siberia. In: Pearson, et al. (Eds.), Proceedings of 10th International Kimberlite Conference, vol. 1. Springer India, New Delhi, pp. 59–74.

Ashchepkov, I.V., Vladykin, N.N., Ntaflos, T., Kostrovitsky, S.I., Prokopiev, S.A., Downes, H., Smelov, A.P., Agashev, A.M., Logvinova, A.M., Kuligin, S.S., Tychkov, N.S., Salikhov, R.F., Stegnitsky, Yu. B., Alymova, N.V., Vavilova, M.A., Minin, V.A., Babushkina, S.A., Ovchinnikov, Yu. I., Karpenko, M.A., Tolstov, A.V., Shmarov, G.P., 2014a. Layering of the lithospheric mantle beneath the Siberian Craton: modeling using thermobarometry of mantle xenolith and xenocrysts. Tectonophysics 634, 55–75.

Ashchepkov, I.V., Alymova, N.V., Logvinova, A.M., Vladykin, N.V., Kuligin, S.S., Mityukhin, S.I., Downes, H., Stegnitsky Yu, B., Prokopiev, S.A., Salikhov, R.F., Palessky, V.S., Khmel'nikova, O.S., 2014b. Picroilmenites in Yakutian kimberlites: variations and genetic models. Solid Earth 5, 915–938.

Ashchepkov, I.V., Kuligin, S.S., Vladykin, N.V., Downes, H., Vavilov, M.A., Nigmatulina, E.N., Babushkina, S.A., Tychkov, N.S., Khmelnikova, O.S., 2016a. Comparison of mantle lithosphere beneath early Triassic kimberlite fields in Siberian craton reconstructed from deep-seated xenocrysts. Geoscience Frontiers 7, 639–662.

Ashchepkov, I.V., Logvinova, A.M., Reimers, L.F., Ntaflos, T., Spetsius, Z.V., Vladykin, N.V., Downes, H., Yudin, D.S., Travin, A.V., Makovchuk, I.V., Palesskiy, V.S., Khmel'nikova, O.S., 2015. The Sytykanskaya kimberlite pipe: evidence from deep-seated xenoliths and xenocrysts for the evolution of the mantle beneath Alakit, Yakutia. Geoscience Frontiers 6, 687–714.

Ashchepkov, I.V., Ntaflos, T., Spetsius, Z.V., Salikhov, R.F., Downes, H., 2016b. Interaction between protokimberlite melts and mantle lithosphere: evidence from mantle xenoliths from the Dalnyaya kimberlite pipe, Yakutia (Russia). Geoscience Frontiers (in press), Accepted Manuscript. http://www.sciencedirect.com/science/article/pii/S1674987116300512.

Aulbach, S., 2012. Craton nucleation and formation of thick lithospheric roots. Lithos 149, 16–30.

Banas, A., Stachel, T., Phillips, D., Shimizu, N., Viljoen, K.S., Harris, J.W., 2009. Ancient metasomatism recorded by ultra-depleted garnet inclusions in diamonds from DeBeers Pool, South Africa. Lithos 112, 736–746.

Bédard, J.H., 2006. A catalytic delamination-driven model for coupled genesis of Archaean crust and sub-continental lithospheric mantle. Geochimica et Cosmochimica Acta 70, 1188–1214.

Brey, G.P., Kohler, T., 1990. Geothermobarometry in four-phase lherzolites. II. New thermobarometers, and practical assessment of existing thermobarometers. Journal of Petrology 31, 1353–1378.

Boyd, F.R., Pokhilenko, N.P., Pearson, D.G., Mertzman, S.A., Sobolev, N.V., Finger, L.W., 1997. Composition of the Siberian cratonic mantle: evidence from Udachnaya peridotite xenoliths. Contributions to Mineralogy and Petrology 128, 228–246.

Bulanova, G.P., Griffin, W.L., Kaminsky, F.V., Davies, R., Ryan, C.G., Andrew, A., Spetsius, Z.V., Zahkarchenko, O.D., 1998. Diamonds from Zarnitsa and Dalnaya kimberlites (Yakutia): their nature, growth history, and lithospheric mantle source. In: Andrewand, A.S., Seccombe, P.K. (Eds.), Proceedings of the VII IKC, pp. 21–24. Edit. Gurney et al.

Chakhmouradian, A.R., 2010. High-field-strength elements in carbonatitic rocks: geochemistry, crystal chemistry and significance for constraining the sources of carbonatites. Chemical Geology 235, 138–160.

Dawson, J.B., 1980. Kimberlites and their Xenoliths. Springer-Verlag, Berlin, 252p.

DePaolo, D.J., 1981. Trace element and isotopic effects of combined wall rock assimilation and fractional crystallization. Earth and Planetary Science Letters 53, 189–202.

Downes, H., de Vries, C., Wittig, N., 2015. Hf -Zr anomalies in clinopyroxene from mantle xenoliths from France and Poland: implications for Lu- Hf dating of spinel peridotite lithospheric mantle. International Journal of Earth Sciences 104, 89–102.

Doucet, L.S., Ionov, D.A., Golovin, A.V., Pokhilenko, N.P., 2012. Depth, degrees and tectonic settings of mantle melting during craton formation: inferences from major and trace element compositions of spinel harzburgite xenoliths from the Udachnaya kimberlite, central Siberia. Earth and Planetary Science Letters 359–360, 206–218.

Doucet, L.S., Peslier, A.H., Ionov, D.A., Brandon, A.D., Golovin, A.V., Goncharov, A.G., Ashchepkov, I.V., 2014. High water contents in the Siberian cratonic mantle linked to metasomatism: an FTIR study of Udachnaya peridotite xenoliths. Geochimica et Cosmochimica Acta 137, 159–187.

Doucet, L.S., Ionov, D.A., Golovin, A.V., 2015. Paleoproterozoic formation age for the Siberian cratonic mantle: Hf and Nd isotope data on refractory peridotite xenoliths from the Udachnaya kimberlite. Chemical Geology 391, 42–55.

Foley, S.F., 2011. A reappraisal of redox melting in the Earth's mantle as a function of tectonic setting and time. Journal of Petrology 52, 1363–1391.

Fishwick, S., 2010. Surface wave tomography: Imaging of the lithosphere–asthenosphere boundary beneath central and southern Africa? Lithos 120, 63–73.

Frezzotti, M.-L., Touret, J.L.R., 2014. CO2, carbonate-rich melts, and brines in the mantle. Geoscience Frontiers 5, 697–710.

Gerya, T., 2014. Precambrian geodynamics: concepts and models. Gondwana Research 25, 442–463.

Gladkochub, D.P., Pisarevsky, S.A., Donskaya, T.V., Natapov, L.M., Mazukabzov, A.M., Stanevich, A.M., Sklyarov, E.V., 2006. Siberian Craton and its evolution in terms of Rodinia hypothesis. Episodes 29, 169–174.

Goncharov, A.G., Ionov, D.A., Doucet, L.S., Pokhilenko, L.N., 2012. Thermal state, oxygen fugacity and C-O-H fluid speciation in cratonic lithospheric mantle: new data on peridotite xenoliths from the Udachnaya kimberlite, Siberia. Earth and Planetary Science Letters 357–358, 99–110.

Green, T.H., Blundy, J.D., Adam, J., Yaxley, G.M., 2000. SIMS determination of trace element partition coefficients between garnet, clinopyroxene and hydrous basaltic liquids at 2–7.5 GPa and 1080–1200°C. Lithos 53, 165–187.

Gregoire, M., Bell, D.R., Le Roex, A.P., 2003. Garnet lherzolites from the Kaapvaal Craton (South Africa): trace element evidence for a metasomatic history. Journal of Petrology 44, 629–657.

Griffin, W.L., O'Reilly, S.Y., 2007. Cratonic lithospheric mantle: is anything subducted? Episodes 30, 43–53.

Griffin, W.L., Ryan, C.G., Kaminsky, F.V., O'Reilly, S.Y., Natapov, L.M., Win, T.T., Kinny, P.D., Ilupin, I.P., 1999a. The Siberian lithosphere traverse: mantle terrains and the assembly of the Siberian Craton. Tectonophysics 310, 1–35.

Griffin, W.L., Shee, S.R., Ryan, C.G., Win, T.T., Wyatt, B.A., 1999b. Harzburgite to lherzolite and back again: metasomatic processes in ultramafic xenoliths from the Wesselton kimberlite, Kimberly, South Africa. Contributions to Mineralogy and Petrology 134, 232–250.

Griffin, W.L., Natapov, L.M., O'Reilly, S.Y., van Achterbergh, E., Cherenkova, A.F., Cherenkov, V.G., 2005. The Kharamai kimberlite field, Siberia: modification of the lithospheric mantle by the Siberian Trap event. Lithos 81, 167–187.

Griffin, W.L., Sobolev, N.V., Ryan, C.G., Pokhilenko, N.P., Win, T.T., Yefimova, E.S., 1993. Trace elements in garnets and chromites: diamond formation in the Siberian lithosphere. Lithos 29, 235–256.

Griffin, W.L., Belousova, E.A., O'Neill, C., O'Reilly, S.Y., Malkovets, V., Pearson, N.J., Spetsius, S., Wilde, S.A., 2014. The world turns over: Hadean–Archean crust–mantle evolution. Lithos 189, 2–15.

Griffin, W.L., Kobussen, A.F., Babu, E.V.S.S.K., O'Reilly, S.Y., Norris, R., Sengupta, P., 2009a. A translithospheric suture in the vanished 1-Ga lithospheric root of South India: evidence from contrasting lithosphere sections in the Dharwar Craton. Lithos 112 (S2), 1109–1119.

Griffin, W.L., O'Reilly, S.Y., Doyle, B.J., Pearson, N.J., Coopersmith, H., Kivi, K., Malkovets, V., Pokhilenko, N., 2004. Lithosphere mapping beneath the North American plate. Lithos 77, 873–922.

Gudmundsson, G., Wood, B., 1995. Experimental tests of garnet peridotite oxygen barometry. Contributions to Mineralogy and Petrology 119, 56–67.

Halla, J., van Hunen, J., Heilimo, E., Holtta, P., 2009. Geochemical and numerical constraints on Neoarchean plate tectonics. Precambrian Research 174, 155–162.

Hanger, B.J., Yaxley, G.M., Berry, A.J., Kamenetsky, V.S., 2015. Relationships between oxygen fugacity and metasomatism in the Kaapvaalsubcratonic mantle, represented by garnet peridotite xenoliths in the Wesselton kimberlite, South Africa. Lithos 212–215, 443–452.

Harte, B., Hunter, R.H., Kinny, P.D., 1993. Melt geometry, movement and crystallization, in relation to mantle dykes, veins and metasomatism. Philosophical Transactions of the Royal Society of London 342, 1–21.

Hart, S.R., Dunn, T., 1993. Experimental cpx/melt partitioning of 24 trace elements. Contributions to Mineralogy and Petrology 113, 1–8.

Horodyskyj, U.N., Lee, C.-T.A., Ducea, M.N., 2007. Similarities between Archean high MgO eclogites and Phanerozoic arc-eclogite cumulates and the role of arcs in Archean continent formation. Earth and Planetary Science Letters 256, 510–520.

Humphreys, E.D., Schmandt, B., Bezada, M.J., Perry-Houts, J., 2015. Recent craton growth by slab stacking beneath Wyoming. Earth and Planetary Science Letters 429, 170–180.

Ilupin, I.P., Vaganov, V.I., Prokopchuk, B.I., 1990. Handbook on Kimberlites. Nedra, Moscow (in Russian).

Ionov, D.A., Doucet, L.S., Carlson, R.W., Golovin, A.V., Korsakov, A.V., 2015. Post-Archean formation of the lithospheric mantle in the central Siberian craton: Re–Os and PGE study of peridotite xenoliths from the Udachnaya kimberlite. Geochimica et Cosmochimica Acta 165, 466–483.

Ionov, D.A., Bénard, A., Plechov, P.Yu., Shcherbakov, V.D., 2013. Along-arc variations in lithospheric mantle compositions in Kamchatka, Russia: first trace element data on mantle xenoliths from the Klyuchevskoy Group volcanoes. Journal of Volcanology and Geothermal Research 263, 122–131.

Ionov, D.A., Doucet, L.S., Ashchepkov, I.V., 2010. Composition of the lithospheric mantle in the Siberian Craton: new constraints from fresh peridotites in the Udachnaya-East Kimberlite. Journal of Petrology 51, 2177–2210.

Ionov, D.A., Doucet, L.S., Carlson, R.W., Pokhilenko, N.P., Golovin, A.V., Ashchepkov, I.V., 2011. Peridotite Xenolith Inferences on the Formation and Evolution of the Central Siberian Cratonic Mantle. Goldschmidt Conference Abstracts. A-1085.

Ivanic, T.J., Nebel, O., Jourdan, F., Faure, K., Kirkland, C.L., Belousova, E.A., 2015. Heterogeneously hydrated mantle beneath the late Archean Yilgarn Craton. Lithos 238, 76–85.

Khar'kiv, A.D., Zuenko, V.V., Zinchuk, N.N. (Eds.), 1991. Kimberlite Geochemistry. Nedra, Moscow (in Russian).

Karato, S., 2010. Rheology of the Earth's mantle: a historical review. Gondwana Research 18, 17–45.

Kopylova, M.G., Nowell, G.M., Pearson, D.G., Markovic, G., 2009. Crystallization of megacrysts from protokimberlitic fluids: geochemical evidence from high-Cr megacrysts in the Jericho kimberlite. Lithos 112, 284–295.

Kostrovitsky, S.I., Morikiyo, T., Serov, I.V., Yakovlev, D.A., Amirzhanov, A.A., 2007. Isotope-geochemical systematics of kimberlites and related rocks from the Siberian Platform. Russian Geology and Geophysics 48 (3), 272–290.

Koreshkova, M.Yu., Downes, H., Nikitina, L.P., Vladykin, N.V., Larionov, A.N., Sergeev, S.A., 2009. Trace element and age characteristics of zircons in granulite xenoliths from the Udachnaya kimberlite pipe, Siberia. Precambrian Research 168, 197–212.

Koulakov, I., Bushenkova, N., 2010. Upper mantle structure beneath the Siberian craton and surrounding areas based on regional tomographic inversion of P and PP travel times. Tectonophysics 486, 81–100.

Kröner, A., Santosh, M., Wong, J., 2012. Zircon ages and Hf isotopic systematics reveal vestiges of Mesoproterozoic to Archaean crust within the late Neoproterozoic–Cambrian high-grade terrain of southernmost India. Gondwana Research 21, 876–886.

Kuligin, S.S., 1997. Complex of Pyroxenite Xenoliths in Kimberlites from Different Regions of Siberian Platform. PhD thesis. United Institute of Geology Geophysics and Mineralogy, Novosibirsk, p. 220.

Kuskov, O.L., Kronrod, V.A., Prokof'ev, A.A., 2011. Thermal structure and thickness of the lithospheric mantle underlying the Siberian Craton from the kraton and kimberlitsuperlong seismic profiles. Izvestiya, Physics of the Solid Earth 47, 55–175.

Lazarov, M., Woodland, A.B., Brey, G., 2009. Thermal state and redox conditions of the Kaapvaal mantle. A study of xenoliths from the Finsch mine, South Africa. Lithos 112, 913–923.

Lee, C.-T.A., Luffi, P., Chin, E.J., 2011. Building and destroying continental mantle. Annual Review of Earth Planetary Sciences 39, 59–90.

Le Roex, A., Class, C., 2016. Metasomatic enrichment of Proterozoic mantle south of the Kaapvaal Craton, South Africa: origin of sinusoidal REE patterns in clinopyroxene and garnet. Contributions to Mineralogy and Petrology 171. http://dx.doi.org/10.1007/s00410-015-1222-8.

Lavrent'ev, Yu.G., Usova, L.V., Kuznetsova, A.I., Letov, S.V., 1987. X-ray spectral quant metric microanalysis of the most important minerals of kimberlites. Russian Geology and Geophysics 48 (5), 75–81.

Lavrent'ev, Yu.G., Usova, L.V., 1994. A new version of the Karat software for quantitative X-ray microanalysis. Zhurnal Analiticheskoi Khimii 46 (5), 462–468.

Logvinova, A.M., Taylor, L.A., Floss, C., Sobolev, N.V., 2005. Geochemistry of multiple diamond inclusions of harzburgitic garnets as examined in situ. International Geology Review 47, 1223–1233.

Ma, X., Fan, H.-R., Santosh, M., Guo, J., 2016. Petrology and geochemistry of the Guyang hornblendite complex in the Yinshan block, North China Craton: implications for the melting of subduction-modified mantle. Precambrian Research 273, 38–52.

Malkovets, V.G., Griffin, W.L., Pearson, N.J., Rezvukhin, D.I., O'Reilly, S.Y., Pokhilenko, N.P., Garanin, V.K., Spetsius, Z.V., Litasov, K.D., 2012. Late Metasomatic Addition of Garnet to the SCLM: Os-isotope Evidence, 10th International Kimberlite Conference Long Abstarcts 10IKC-173.

Maruyama, S., Ikoma, M., Genda, H., Hirose, K., Yokoyama, T., Santosh, M., 2012. The naked planet Earth: most essential pre-requisite for the origin and evolution of life. Geoscience Frontiers 2, 141–165.

Maruyama, S., Okamoto, K., 2007. Water transportation from the subducting slab into the mantle transition zone. Gondwana Research 11, 148–165.

McCammon, C.A., Griffin, W.L., Shee, S.R., O'Neill, H.S.C., 2001. Oxidation during metasomatism in ultramafic xenoliths from the Wesselton kimberlite, South Africa: implications for the survival of diamond. Contributions to Mineralogy and Petrology 141, 287–296.

McDonough, W.F., Sun, S.S., 1995. The composition of the Earth. Chemical Geology 120 (3–4), 223–253.

Please cite this article in press as: Ashchepkov, I.V., et al., Alakit and Daldyn kimberlite fields, Siberia, Russia: Two types of mantle sub-terranes beneath central Yakutia?, Geoscience Frontiers (2016), http://dx.doi.org/10.1016/j.gsf.2016.08.004

McGregor, I.D., 1974. The system $MgO–Al_2O_3–SiO_2$: solubility of Al_2O_3 in enstatite for spinel and garnet–spinel compositions. American Mineralogist 59, 110–190.
McKenzie, D., Priestley, K., 2008. The influence of lithospheric thickness variations on continental evolution. Lithos 102, 1–11.
Nance, R.N., Murphy, J.B., Santosh, M., 2014. The supercontinent cycle: a retrospective essay. Gondwana Research 25, 4–29.
Nimis, P., Zanetti, A., Dencker, I., Sobolev, N.V., 2009. Major and trace element composition of chromian diopsides from the Zagadochnaya kimberlite (Yakutia, Russia): metasomatic processes, thermobarometry and diamond potential. Lithos 112 (3–4), 397–412.
Nimis, P., Taylor, W., 2000. Single clinopyroxene thermobarometry for garnet peridotites. Part I. Calibration and testing of a Cr-in-Cpx barometer and an enstatite-in-Cpx thermometer. Contributions to Mineralogy and Petrology 139, 541–554.
Nixon, P.H., Boyd, F.R., 1973. Petrogenesis of the granular and sheared ultrabasic nodulesuite in kimberlite. In: Nixon, P.H. (Ed.), Lesotho Kimberlites. Cape and Transvaal, Maseru, pp. 48–56.
Ntaflos, Th., Bjerg, E.A., Labudia, C.H., Kurat, G., 2007. Depleted lithosphere from the mantle wedge beneath Tres Lagos, southern Patagonia, Argentina. Lithos 94, 46–65.
O'Neill, H. St. C., Wall, V.J., 1987. The olivine orthopyroxene-spinel oxygen geobarometer, the nickel precipitation curve, and the oxygen fugacity of the Earth's upper mantle. Journal of Petrology 28, 1169–1191.
O'Neill, H.St.C., Wood, B.J., 1979. An experimental study of Fe-Mg- partitioning between garnet and olivine and its calibration as a geothermometer. Contributions to Mineralogy and Petrology 70, 59–70.
O'Reilly, S.Y., Zhang, M., Griffin, W.L., Begg, G., Hronsky, J., 2009. Ultradeep continental roots and their oceanic remnants: a solution to the geochemical "mantle reservoir" problem? Lithos 112 (S1), 1043–1054.
O'Reilly, S.Y., Griffin, W.L., 2010. The continental lithosphere–asthenosphere boundary: can we sample it? Lithos 120, 1–13.
Pavlenkova, N.I., 2011. Seismic structure of the upper mantle along the long-range PNE profiles — rheological implication. Tectonophysics 508, 85–95.
Pearson, D.G., Snyder, G.A., Shirey, S.B., Taylor, L.A., Carlson, R.W., Sobolev, N.V., 2005. Archaean Re–Os age for Siberian eclogites and constraints on Archaean tectonics. Nature 374, 711–713.
Pearson, D.G., 1999. The age of continental roots. Lithos 48, 171–194.
Pedersen, H.A., Debayle, E., Maupin, V., POLENET/LAPNET Working Group, 2013. Strong lateral variations of lithospheric mantle beneath cratons – example from the Baltic Shield. Earth and Planetary Science Letters 383, 164–172.
Pernet-Fisher, J.F., Howarth, G.H., Liu, Y., Barry, P.H., Carmody, L., Valley, J.W., Bodnar, R.J., Spetsius, Z.V., Taylor, L.A., 2014. Komsomolskaya diamondiferous eclogites: evidence for oceanic crustal protoliths. Contributions to Mineralogy and Petrology 167, 981. http://dx.doi.org/10.1007/s00410-014-0981-y.
Peslier, A.H., Woodland, A.B., Bell, D.R., Lazarov, M., 2010. Olivine water contents in the continental lithosphere and the longevity of cratons. Nature 467, 78–81.
Piper, J.A.D., 2010. Protopangaea: palaeomagnetic definition of Earth's oldest (mid-Archaean-Palaeoproterozoic) supercontinent. Journal of Geodynamics 50, 154–165.
Pokhilenko, L.N., Alifirova, T.A., Yudin, D.S., 2013. $^{40}Ar/^{39}Ar$-dating of phlogopite from mantle xenoliths: evidence for deep ancient metasomatism of the Siberian craton lithosphere. Doklady Earth Sciences 449, 309–312.
Pokhilenko, N.P., Sobolev, N.V., Kuligin, S.S., Shimizu, N., 1999. Peculiarities of distribution of pyroxenite paragenesis garnets in Yakutian kimberlites and some aspects of the evolution of the Siberian craton lithospheric mantle. In: Proceedings of the VII International Kimberlite Conference. The P.H. Nixon volume, pp. 690–707.
Pokhilenko, N.P., Pearson, D.G., Boyd, F.R., Sobolev, N.V., 1991. Megacrystalline dunites: sources of Siberian diamonds, vol. 90. Carnegie Institute Washington. Yearbook, pp. 11–18.
Pokhilenko, N.P., Sobolev, N.V., Sobolev, V.S., Lavrentiev, Yu.G., 1976. Xenolith of diamond bearing ilmenite-pyrope lherzolite from the Udachnaya kimberlite pipe, Yakutia. Doklady Earth Sciences 231, 149–151.
Roberts, N.M.W., Van Kranendonk, M.J., Parman, S., Clift, P.D., 2015. Continent formation through time. In: Roberts, N.M.W., Van Kranendonk, M.J., Parman, S., Shirey, S., Clift, P.D. (Eds.), Continent Formation Through Time, pp. 1–16. Geological Society, London, Special publication 389.
Roberts, N.M.W., Spencer, C.J., 2015. The zircon archive of continent formation through time. In: Roberts, N.M.W. (Ed.), Continent Formation Through Time, vol. 389. Geological Society of London, Special Publications, London, UK, pp. 197–225.
Riches, A.J.V., Liu, Y., Day, J.M.D., Spetsius, Z.V., Taylor, L.A., 2010. Subducted oceanic crust as diamond hosts revealed by garnets of mantle xenoliths from Nyurbinskaya, Siberia. Lithos 120, 368–378.
Rodionov, A.S., Amshinsky, A.N., Pokhilenko, N.P., 1988. Ilmenite–pyrope wehrlite — a new type of kimberlite xenoliths paragenesis. Russian Geology and Geophysics 19/7, 53–57.
Rollinson, H.R., 1993. Using Geochemical Data: Evaluation, Presentation, Interpretation. Longman, Harlow, England, 290 pp.
Rosen, O.M., Levskii, L.K., Makeev, A.F., Zhuravlev, D.Z., Spetsius, Z.V., Rotman, A.Ya., Zinchuk, N.N., Manakov, A.V., Serenko, V.P., 2006. Paleoproterozoic accretion in the Northeast Siberian craton: isotopic dating of the Anabar collision system. Stratigraphy and Geological Correlation 14, 581–601.
Rosen, O.M., Manakov, A.V., Suvorov, V.D., 2005. The collisional system in the northeastern Siberian craton and a problem of diamond-bearing lithospheric keel. Geotectonics 39, 456–479.
Rudnick, R.L., McDonough, W.F., O'Connell, R.J., 1998. Thermal structure, thickness and composition of continental lithosphere. Chemical Geology 145, 395–411.
Sand, K.K., Waight, T.E., Pearson, D.G., Nielsen, T.F.D., Makovicky, E., Hutchison, M.T., 2009. The lithospheric mantle below southern West Greenland: a geothermobarometric approach to diamond potential and mantle stratigraphy. Lithos 112, 1155–1166.
Santosh, M., 2010. A synopsis of recent conceptual models on supercontinent tectonics in relation to mantle dynamics, life evolution and surface environment. Journal of Geodynamics 116–133.
Santosh, M., Maruyama, S., Yamamoto, S., 2009. The making and breaking of supercontinents: some speculations based on superplumes, super downwelling and the role of tectosphere. Gondwana Research 15, 324–341.
Salikhov, R.F., Ivanyushina, E.N., Gritsenko, A.V., 2015. Structural and Tectonic Criteria in Large-scale, Local Forecasting in the Closed Area (Example of Alakit-Markha Field). Abstracts of the scientific- practical conference on Diamond prospecting. Aykhal, Russia, pp. 146–154 (in Russian).
Shatsky, V., Ragozin, A., Zedgenizov, D., Mityukhin, S., 2008. Evidence for multistage evolution in a xenolith of diamond-bearing eclogite from the Udachnaya kimberlite pipe. Lithos 105, 289–300.
Shu, Q., Brey, G.P., 2015. Ancient mantle metasomatism recorded in subcalcic garnet xenocrysts: temporal links between mantle metasomatism, diamond growth and crustal tectonomagmatism. Earth and Planetary Science Letters 418, 27–39.
Smith, C.B., Pearson, D.G., Bulanova, G.P., Beard, A.D., Carlson, R.W., Wittig, N., Sims, K., Muchemwa, E., 2009. Extremely depleted lithospheric mantle and diamonds beneath the southern Zimbabwe Craton. Lithos 112, 1120–1132.
Snyder, G.A., Taylor, L.A., Crozaz, G., Halliday, A.N., Beard, B.L., Sobolev, V.N., 1997. The origins of Yakutian eclogite xenoliths. Journal of Petrology 38, 85–113.
Snyder, D.B., Lockhart, G., 2009. Does seismically anisotropic subcontinental mantle lithosphere require metasomatic wehrlite–pyroxenite dyke stockworks? Lithos 112, 961–965.
Sobolev, S.V., Sobolev, A.V., Kuzmin, D.V., Krivolutskaya, N.A., Petrunin, A.G., Arndt, N.T., Radko, V.A., Vasiliev, Y.R., 2011. Linking mantle plumes, large igneous provinces and environmental catastrophes. Nature 477, 312–316.
Sobolev, N.V., Pokhilenko, N.V., Efimova, E.S., 1984. Xenoliths of diamond bearing peridotites in kimberlites and problem of the diamond origin. Russian Geology and Geophysics 25/12, 63–80.
Sobolev, N.V., 1977. Deep-seated Inclusions in Kimberlites and the Problem of the Composition of the Mantle. Amer. Geophys. Union, Washington, DC, p. 279.
Sobolev, N.V., Logvinova, A.M., Zedgenizov, D.A., Seryotkin, Y.V., Yefimova, E.S., Floss, C., Taylor, L.A., 2004. Mineral inclusions in microdiamonds and macrodiamonds from kimberlites of Yakutia: a comparative study. Lithos 77, 225–242.
Sobolev, N.V., Lavrentev, Y.G., Pokhilenko, N.P., Usova, L.V., 1973. Chrome-rich garnets from the kimberlites of Yakutia and their parageneses. Contributions to Mineralogy and Petrology 40, 39–52.
Sobolev, N.V., Sobolev, A.V., Tomilenko, A.A., Kovyazin, S.V., Batanova, V.G., Kuz'min, D.V., 2015. Paragenesis and complex zoning of olivine macrocrysts from unaltered kimberlite of the Udachnaya-East pipe, Yakutia: relationship with the kimberlite formation conditions and evolution. Russian Geology and Geophysics 56, 260–279.
Sobolev, V.N., Sobolev, N.V., 1993. Nd and Sr isotopes from diamondiferous eclogites, Udachnaya kimberlite pipe, Yakutia, Siberia: evidence of differentiation in the early Earth? Earth and Planetary Science Letters 118, 91–100.
Sobolev, N.V., Sobolev, V.N., Snyder, G.A., Yefimova, E.S., Taylor, L.A., 1999. Significance of eclogitic and related parageneses of natural diamonds. International Geology Review 129–140.
Spandler, C., Hermann, J., Arculus, R., Mavrogenes, J., 2004. Geochemical heterogeneity and element mobility in deeply subducted oceanic crust; insights from high-pressure mafic rocks from New Caledonia. Chemical Geology 206, 21–42.
Spetsius, Z.V., Serenko, V.P., 1990. Composition of the Continental Mantle and Low Crust beneath the Siberian Platform. Nauka, Moscow, 271 p (in Russian).
Spetsius, Z.V., Taylor, L.A., Valley, J.W., DeAngelis, M.T., Spicuzza, M., Ivanov, A.S., Banzeruk, V.I., 2008. Diamondiferous xenoliths from crustal subduction: garnet oxygen isotopes from the Nyurbinskaya pipe, Yakutia. European Journal of Mineralogy 20, 375–385.
Spetsius, Z.V., Koptil, V.I., 2008. Associations with the diamond from the kimberlite pipe Sytykanskaya, Yakutia. Geologiya I Razvedka 23–28.
Stachel, T., Harris, J.W., 2008. The origin of cratonic diamonds –constraints from mineral inclusions. Ore Geology Reviews 34 (1–2), 5–32.
Stagno, V., Ojwang, D.O., McCammon, C.A., Frost, D.J., 2013. The oxidation state of the mantle and the extraction of carbon from Earth's interior. Nature 493, 84–88.
Sun, J., Liu, C.-Z., Tappe, S., Kostrovitsky, S.I., Wu, F.-Y., Yakovlev, D., Yang, Y.-H., Yang, H., 2014. Repeated kimberlite magmatism beneath Yakutia and its relationship to Siberian flood volcanism: insights from in situ U–Pb and Sr–Nd perovskite isotope analysis. Earth and Planetary Science Letters 404, 283–295.
Thybo, H., Artemieva, I.M., 2013. Moho and magmatic underplating in continental lithosphere. Tectonophysics 609, 605–619.
Taylor, W.R., Kammerman, M., Hamilton, R., 1998. New Thermometer and Oxygen Fugacity Sensor Calibrations for Ilmenite and Chromium Spinel-bearing

Please cite this article in press as: Ashchepkov, I.V., et al., Alakit and Daldyn kimberlite fields, Siberia, Russia: Two types of mantle sub-terranes beneath central Yakutia?, Geoscience Frontiers (2016), http://dx.doi.org/10.1016/j.gsf.2016.08.004

Peridotitic Assemblages, 7th International Kimberlite Conference. Extended abstracts. Cape Town, pp. 891–901.
van Hunen, J., van den Berg, A.P., 2008. Plate tectonics on the early Earth: limitations imposed by strength and buoyancy of subducted lithosphere. Lithos 103, 217–235.
Wittig, N., Pearson, D.G., Webb, M., Ottley, C.J., Irvine, G.J., Kopylova, M., Jensen, S.M., Nowell, G.M., 2008. Origin of cratonic lithospheric mantle roots. A geochemical study of peridotites from the North Atlantic Craton, West Greenland. Earth and Planetary Science Letters 274, 24–33.
Zhao, X.-M., Zhang, H.-F., Zhu, X.-K., Zhu, B., Cao, H.-H., 2015. Effects of melt percolation on iron isotopic variation in peridotites from Yangyuan, North China Craton. Chemical Geology 401, 96–110.
Zaitsev, A.I., Smelov, A.P., 2010. Isotopic Geochronology of the Species of the Kimberlitic Formation of Yakut Province. Yakutsk 105 p.
Zinchuk, N.N., Spetsius, Z.V., Zuenko, V.V., Zuev, V.M., 1993. Udachnaya Kimberlite Pipe: Composition and Formation Conditions. Izd. Novosibirsk. Gos. Univ., Novosibirsk (in Russian).

Please cite this article in press as: Ashchepkov, I.V., et al., Alakit and Daldyn kimberlite fields, Siberia, Russia: Two types of mantle sub-terranes beneath central Yakutia?, Geoscience Frontiers (2016), http://dx.doi.org/10.1016/j.gsf.2016.08.004